Implications of high-Mg# adakitic magmatism at Hunter Ridge for arc magmatism of the Fiji - Vanuatu Region

McCarthy, A.[1,2*], Falloon, T. J.[3], Danyushevsky L. V. [3], Sauermilch, I.[1,4], Patriat, M. [5], Jean, M. M. [6,7], Maas, R. [8], Woodhead, J. D. [8], G.M. Yogodzinski[9]

[1]Institute of Marine and Antarctic Studies, University of Tasmania, Australia

[2] Institute of Geochemistry and Petrology, ETH Zurich, Switzerland

[3] CODES and Earth Sciences, School of Natural Sciences, University of Tasmania, Australia

[4] Department of Earth Sciences, Faculty of Geosciences, Utrecht University, Utrecht, The Netherlands

[5] Geo-Ocean, Univ Brest, CNRS, Ifremer, UMR6538, F-29280 Plouzané, France

[6] Western Colorado University, Department of Geology, 1 Western Way, Hurst Hall 128, Gunnison, CO 81231

[7] Ohio University, Lancaster, 1570 Granville Pike, Lanaster, OH 43130

[8] School of Earth Sciences, University of Melbourne, Victoria 3010, Australia

[9] School of the Earth, Ocean, and Environment, University of South Carolina, USA

*E-mail: anders.mccarthy@erdw.ethz.ch

Contents: Analytical methods, additional figure as well as major-, trace-, and isotopic element data for dredged volcanic rocks.

DR1: Map of the Aleutians subdivided into western Aleutians (black letters) and Eastern Aleutians (gray letters). After Yogodzinski et al., (2015). Bathymetry from Weatherall et al. (2015); **DR2: A-B)** Hf-Nd isotopic composition of Hunter Ridge lavas; **C)** Sr (ppm) as a function of $^{87}Sr/^{86}Sr$ (as in Fig.8 of the main text), with mixing lines showing the effect of slab melts on Sr abundances and isotopic composition. Addition of a slab melt to a DMM leads to strongly variable Sr abundances at unradiogenic $^{87}Sr/^{86}Sr$ whilst addition of sediment melt or AOC to a DMM leads to a rapid increasing radiogenic $^{87}Sr/^{86}Sr$ at low Sr abundances. Data as in **Fig.9** and **Table 1** of the main text; **DR3: Fig. DR3:** This figure illustrates the evolution of REE patterns as a function of amphibole fractionation. Starting compositions are average low-K_2O and medium-K_2O arc lavas from the Monzier Rift (data from Patriat et al., 2019). Increments of 30% and 50% amphibole fractionation are shown (assuming constant amphibole-melt Kds of ca. 950°C from Nandekar et al., 2016). Chondrite values are from McDonough and Sun, (1995). Amphibole fractionation will induce trough-like REE patterns, with a decrease in MREE/HREE and only limited increase in LREE/MREE. This is illustrated by the change in Dy/Yb ratio, which gradually diminishes (from 1.9 to 1.3) with increasing amphibole fractionation. Instead, Hunter Ridge and Kadavu adakitic rocks have Gd/Yb (1.5 – 5.7) and Dy/Yb (1.6 – 3.0), whilst also preserving high-Mg# bulk rock compositions. **DR4:** Estimated thickness of sediments along the South Fiji Basin; total sediment thickness from Straume et al. (2019) and bathymetry from Weatherall et al. (2015); **DR5:** Characteristics of dredged samples used for this study. Samples vary from fresh to slightly altered sparsely phyric massive flows to highly olivine phyric lava flows and finally to quenched pillow margins with preserved volcanic glass. Although phenocryst abundances vary significantly from one sample to another, they are typically dominated by mm-sized olivine containing spinel inclusions, as well as clinopyroxene and plagioclase phenocrysts. Orthopyroxene phenocrysts are also present in high-Mg# adakites, whilst amphibole remains rather sparse. See Patriat et al., 2019 (supplementary appendix) for images of dredged rocks and thin section images of highly vesicular adakitic rock and sparsely phyric, fine-grained back-arc basalt from Hunter Ridge and Monzier Rift. Description of high-Mg adakitic rocks from Kadavu can be found in Danyushevsky et al., (2008) (supplementary appendix); **DR6:** Major element dataset of dredged volcanic rock; **DR7**: Trace element dataset of dredged volcanic rocks; **DR8**:

Sr-Nd-Hf-Pb isotopic dataset of dredged adakitic volcanic rocks, **DR9**: Sr-Nd isotopic dataset of Monzier Rift back-arc basalts and low- to medium K_2O arc lavas (Patriat et al., 2019)

1. Detailed Analytical Methods

Analyses of glasses were acquired on a Cameca SX100 electron microprobe equipped with 5 wavelength dispersive spectrometers at the Central Science Laboratory, University of Tasmania. Operating conditions were 40 degrees takeoff angle, beam energy of 15 keV, beam current of 20 nA, and 30 microns beam diameter. Elements were acquired using analyzing crystals LLIF (Fe ka, Mn ka, Ti ka, Cr ka, Ni ka), LPET (P ka, K ka, Ca ka), and TAP (Al ka, Si ka, Na ka, Mg ka). The standards were Bustamite (Mn), Hematite (Fe), Rutile (Ti), Nickel Silicide (Ni), Clinopyroxene Delegate (Si, Ca), San Carlos Olivine USNM111312/444 (Mg), Labradorite USNM115900 (Al), Chromite Tiebaghi USNM117075 (Cr), Anorthoclase Kakanui USNM133868 (Na), Microcline (K) and Apatite Durango (P). Peak counting time were 10 s for Na, Mn, Ti, K, Ca, Si, Cr, 20 s for P, 30 s for Fe, and 50 s for Mg, Al, Ni. Off peak counting time was 10 s for Na, Mn, Ti, K, Ca, P, Si, Cr, 20 s for Fe, and 50 s for Mg, Al, Ni. Off Peak correction method was Linear for Na, Mg, Fe, Ti, K, Ca, Al, Si, Cr, Ni, and Slope (Hi) for Mn, P. Unknown and standard intensities were corrected for deadtime. Standard intensities were corrected for standard drift over time. Interference corrections were applied to Mn for interference by Cr (Donovan et al., 1993). Detection limits ranged from .007 wt% for Al to .012 wt% for K to .018 weight percent for Ni to .031 wt% for Na ka to .037 wt% for Ti ka. Analytical sensitivity (at the 99% confidence level) ranged from .286 % relative for Al to .545 % relative for Mg to 2.165 % relative for Na to 14.059 %relative for P to 331.650 % relative for Cr. Oxygen was calculated by cation stoichiometry and included in the matrix correction. The matrix correction method was ZAF or Phi-Rho-Z (Armstrong, 1988). Correction factors were derived from the analysis of international standard USNM 111240/2 (basaltic glass) from Jarosewich et al. (1980), which were applied to the glass analyses.

Glass trace element abundances were determined at CODES Analytical

Laboratories at the University of Tasmania using an Agilent 7500cs quadrupole ICP-MS coupled to a RESOlution HR laser ablation microprobe equipped with a 193 nm Coherent COMPex Pro ArF Excimer Laser and an S155 ablation cell with constant geometry design. A flow of He carrier gas at a rate of 0.35 l/min carried aerosols ablated by the laser out of the chamber to be mixed with Ar gas and carried to the plasma torch. A 110 µm spot size was used for ablation. NIST612 was used as the calibration reference material (Jochum et al., 2008) and Ca as the Internal Standard element. Both BCR-2g and GSD-1g (Jochum et al., 2008) were used as secondary reference materials for quality monitoring. Both primary and secondary reference materials were analysed at the beginning and end of each batch to correct for instrument drift. Data quantification was performed using an in-house data reduction spreadsheet.

For bulk rock chemistry, samples were ground in an agate mill to avoid trace element contamination. Major element analyses were performed at CODES Analytical Laboratories at the University of Tasmania using X-ray fluorescence spectrometry (XRF) and the methods of Robinson (2003). Whole rock sample powders were fused with 12-22 flux (a pre-fused mixture consisting of 12 parts $Li_2B_4O_7$ and 22 parts $LiBO_2$) using a sample:flux ratio of 1:9 at 1100˚C. All fusions are performed in a non-wetting 5% Au-95% Pt alloy crucible. The following quantities are used to make 32 mm diameter discs: 12-22 flux (4.5000 g), sample (0.5000 g) and $LiNO_3$ (0.0606 g, added as 100µl of 60.6% $LiNO_3$). The mix is fused with agitation at 1100˚C for 15 minutes before being cast in a 5% Au -95% Pt mould. Ignition loss was determined on ~2 grams of sample powder ignited overnight at 1000˚C in 5ml platinum crucibles. Major elements were determined with a ScMo 3kW side window X-ray tube and a Philips PW1480 x-ray spectrometer. Corrections for mass absorption are calculated using Philips X40 software with De Jongh's calibration model and Philips (or CSIRO) alpha coefficients. Compton scattering is also used for many trace elements. Calibrations are on pure element oxide mixes in pure silica, along with international and Tasmanian standard rocks are used. Trace elements were determined by using pressed powder pill analysis (10grams, 32mm) using a combination of ScMo (Y, Rb, Ni) and Au (Ba, Nb, La, Ce, Sr, Zr, V, Sc, Cr) 3kW side window X-ray tubes and a Philips PW1480 x-ray spectrometer.

Additional trace elements were also acquired by solution ICP-MS at CODES Analytical Laboratories using the methods of Robinson et al. (1999) and Yu et al. (2000). ICP-MS analyses were performed on duplicate high-pressure HF-H_2SO_4-$HClO_4$ digestions. Sub-boiling double distilled acids and ultra pure water were used, as were clean sampler and skimmer cones, ICP torch, spray chamber, nebuliser and sample introduction tubes (including auto-sampler tubing). Prior to sample analysis the instrument was purged for at least 24 hours with 5% v/v HNO_3 rinse solution.

Radiogenic isotope ratios were determined at the University of Melbourne, following procedures described in Woodhead (2002), Maas et al. (2005) and Yaxley et al. (2013). Approx. 100 mg of handpicked chips or rock powders (milled in agate), in some cases both, were leached with 6M HCl (100°C, 60 min), rinsed with distilled water, and digested on a hotplate (2 days 3:1 HF/HNO3). After centrifuging, the HF-HNO_3 supernatant solution was removed, dried, repeatedly refluxed with concentrated HNO_3, re-dissolved in 3M HCl and loaded onto 1 ml EICHROM LN resin columns for extraction of Hf (Münker et al., 2001). The complementary solid fluoride fraction was re-dissolved in 0.6M HBr and loaded onto a 0.1 ml column of anion resin (AG-1X8, 100-200 mesh) for separation of Pb. The HBr eluate was captured, dried, refluxed with HNO_3 and used for extraction of Sr and Nd on small columns of EICHROM SR-, RE- and LN-resin, respectively. Total analytical blanks (~50 pg for Pb and Hf; ≤100 pg for Nd and Sr) are negligible compared to the amounts of Pb, Hf, Nd and Sr processed. All isotopic analyses were carried out on a Nu Plasma multi-collector ICP-MS with sample introduction via a low-uptake Glass Expansion PFA nebuliser and a CETAC Aridus desolvator. Typical sensitivity in this set-up is in the range of 100-150 V/ppm Sr, Nd, Pb or Hf. Instrumental mass bias was corrected by normalizing to $^{146}Nd/^{145}Nd$ = 2.0719425 (equivalent to $^{146}Nd/^{144}Nd$ = 0.7219), $^{86}Sr/^{88}Sr$ = 0.1194 and $^{179}Hf/^{177}Hf$=0.7325, using the exponential law. Data are reported relative to La Jolla Nd = 0.511860, SRM987 = 0.710230 and JMC475 = 0.282160. Results for international standards, including BCR2 ($^{143}Nd/^{144}Nd$ = 0.512637, n = 7) (Raczek et al., 2003), BHVO2 ($^{86}Sr/^{88}Sr$ = 0.703448, n = 2) (Raczek et al., 2003), Eimer and Amend $SrCO_3$ standard ($^{86}Sr/^{88}Sr$=0.707988, n=5) (Jones et al., 1994) are consistent with TIMS and MC-ICPMS reference values. Typical in-run precision (2 standard error) is ±0.00001 (Nd), ±0.000016 (Sr) and ±0.000008 (Hf).

External (2 standard deviation) precision is ±0.000028, ±0.000012 and ±0.000015, respectively. Mass bias for Pb was corrected using the thallium-doping technique described in Woodhead (2002). This produces data with an external precision (2 standard deviation) of ±0.04-0.06% for $^{206}Pb/^{204}Pb$ and $^{207}Pb/^{204}Pb$, and 0.07-0.09% for $^{208}Pb/^{204}Pb$. Repeat analysis of BCR2 gives values of 18.760 for $^{206}Pb/^{204}Pb$, 15.621 for $^{207}Pb/^{204}Pb$ and 38.735 for $^{208}Pb/^{204}Pb$ (n=7), consistent with published data (e.g. Woodhead and Hergt, 2000, Elburg et al., 2005). Parent/daughter ratios for age corrections are derived from trace element data for unleached sample powders and have precisions of 2-3%.

2. References

Armstrong, J. T., 1988. Quantitative analysis of silicates and oxide minerals: Comparison of Monte-Carlo, ZAF and Phi-Rho-Z procedures, Microbeam Analysis, 239-246

Danyushevsky, L.V., Falloon, T.J., Crawford, A.J., Tetroeva, S.A., Leslie, R.L. and Verbeeten, A., 2008. High-Mg adakites from Kadavu Island Group, Fiji, southwest Pacific: Evidence for the mantle origin of adakite parental melts. Geology, 36(6), 499-502.

Donovan, J.J., Snyder D.A., and Rivers, M.L. 1993. An Improved Interference Correction for Trace Element Analysis in Microbeam Analysis, 2, 23-28

Elburg, M., Vroon, P., van der Wagt, B. and Tchalikian, A., 2005. Sr and Pb isotopic composition of five USGS glasses (BHVO-2G, BIR-1G, BCR-2G, TB-1G, NKT-1G). Chemical Geology, v. 223(4), p.196-207

Jarosewich, E., Nelen, J.A. and Norberg, J.A., 1980. Reference samples for electron microprobe analysis. Geostandards Newsletter, 4(1), 43-47

Jochum, K. P., and Stoll, B. I., 2008. Reference materials for elemental and isotopic analyses by LA- (MC)-ICP-MS: successes and outstanding needs. In: Sylvester, P. (ed.). Laser Ablation ICPMS in the Earth Sciences: Current practices and outstanding issues. Mineralogical Association of Canada. Short Course v. 40, p.147-168.

Jones, C.E., Jenkyns, H.C., Coe, A.L. and Stephen, H.P., 1994. Strontium isotopic variations in Jurassic and Cretaceous seawater. Geochimica et Cosmochimica Acta, 58(14), p. 3061-3074, https://doi.org/10.1016/0016-7037(94)90179-1

McDonough, W.F., Sun, S-s., 1995. The composition of the Earth, Chemical Geology, 120, p. 223-253.

Müller, R.D., Seton, M., Zahirovic, S., Williams, S.E., Matthews, K.J., Wright, N.M., Shephard, G.E., Maloney, K.T., Barnett-Moore, N., Hosseinpour, M. and Bower, D.J., 2016. Ocean basin evolution and global-scale plate reorganization events since Pangea breakup. Annual Review of Earth and Planetary Sciences, 44, p.107-138.

Münker, C., Weyer, S., Scherer, E. and Mezger, K., 2001. Separation of high field strength elements (Nb, Ta, Zr, Hf) and Lu from rock samples for MC-ICPMS measurements. Geochemistry, Geophysics, Geosystems, 2(12), https://doi.org/10.1029/2001GC000183

Nandedkar, R.H., Hürlimann, N., Ulmer, P., and Müntener, O., 2016. Amphibole–melt trace element partitioning of fractionating calc-alkaline magmas in the lower crust: an experimental study. Contributions to Mineralogy and Petrology, 171:71 https://doi.org/10.1007/s00410-016-1278-0

Patriat, M., Falloon, T., Danyushevsky, L., Collot, J., Jean, M.M., Hoernle, K., Hauff, F., Maas, R., Woodhead, J.D. and Feig, S.T., 2019. Subduction initiation terranes exposed at the front of a 2 Ma volcanically-active subduction zone. Earth and Planetary Science Letters, v. 508, p. 30-40, https://doi.org/10.1016/j.epsl.2018.12.011

Robinson, P., Townsend, A. T., Yu, Z., and Münker, C., 1999. Determination of Scandium, Yttrium and Rare Earth Elements in rocks by high resolution inductively coupled plasmamass spectrometry, Geostandards Newsletter, v.23, p. 31-46.

Robinson, P. 2003, XRF analysis of flux-fused discs, paper presented at Geoanalysis 2003: The 5th International Conference on the Analysis of Geological and Environmental Materials, Geological Survey of Finland, Rovaniemi, Finland.

Straume, E.O., Gaina, C., Medvedev, S., Hochmuth, K., Gohl, K., Whittaker, J.M., Abdul Fattah, R., Doornenbal, J.C. and Hopper, J.R., 2019. GlobSed: Updated total sediment thickness in the world's oceans. Geochemistry, Geophysics, Geosystems, 20(4), p.1756-1772.

Weatherall, P., Marks, K.M., Jakobsson, M., Schmitt, T., Tani, S., Arndt, J.E., Rovere, M., Chayes, D., Ferrini, V. and Wigley, R., 2015. A new digital bathymetric model of the world's oceans. Earth and Space Science, 2(8), p.331-345.

Woodhead, J.D. and Hergt, J.M., 2000. Pb-isotope analyses of USGS reference materials. Geostandards Newsletter, v. 24(1), p. 33-38.

Woodhead, J.D. 2002, A simple method for obtaining highly accurate Pb isotope data by MC-ICP-MS. Journal of Analytical Atomic Spectrometry, v. 17,p. 1-6.

Yaxley, G.M., Kamenetsky, V.S., Nichols, G.T., Maas, R., Belousova, E., Rosenthal, A. and Norman, M., 2013. The discovery of kimberlites in Antarctica extends the vast Gondwanan Cretaceous province. Nature Communications, v. 4(1), p. 1-7, https://doi.org/10.1038/ncomms3921

Yu Z., P. Robinson, A. T. Townsend, C. Münker, and A. J. Crawford 2000. Determination of HFSE, Rb, Sr, Mo, Sb, Cs, Tl and Bi at ng g-1 levels in geological reference materials by magnetic sector ICP-MS after HF/HCLO4 high pressure digestion, Geostandards Newsletter, v. 24, p. 39-50.

3. Data compilations

2.1 Vanutu arc

Beaumais, A., Chazot, G., Dosso, L. and Bertrand, H., 2013. Temporal source evolution and crustal contamination at Lopevi Volcano, Vanuatu Island Arc. Journal of volcanology and geothermal research, v. 264, p. 72-84, https://doi.org/10.1016/j.jvolgeores.2013.07.005

Beaumais, A., Bertrand, H., Chazot, G., Dosso, L. and Robin, C., 2016. Temporal magma source changes at Gaua volcano, Vanuatu island arc. Journal of Volcanology and Geothermal Research, v. 322, p. 30-47,

https://doi.org/10.1016/j.jvolgeores.2016.02.026

Beier, C., Brandl, P.A., Lima, S.M. and Haase, K.M., 2018. Tectonic control on the genesis of magmas in the New Hebrides arc (Vanuatu). Lithos, v. 312, p. 290-307, https://doi.org/10.1016/j.lithos.2018.05.011

Briqueu, L. and Lancelot, J.R., 1983. Sr isotopes and K, Rb, Sr balance in sediments and igneous rocks from the subducted plate of the Vanuatu (New Hebrides) active margin. Geochimica et Cosmochimica Acta, v. 47(2), p. 191-200, https://doi.org/10.1016/0016-7037(83)90132-1

Briqueu, L., Laporte, C., Crawford, A.J., Hasenaka, T., Baker, P.E. and Coltorti, M., 1994. Temporal magmatic evolution of the Aoba basin, central New Hebrides island arc: Pb, Sr and Nd isotopic evidence for the coexistence of two mantle components beneath the arc, in Green, H.G., Collot, J.-Y., Stokking, L.B., et al., 1994, Proceedings of the Ocean Drilling Program, Scientific Results, v.134, p. 393-401

Crawford, A.J., Briqueu, L., Laporte, C. and Hasenaka, T., 1995. Coexistence of Indian and Pacific oceanic upper mantle reservoirs beneath the central New Hebrides island arc. Active Margins and Marginal Basins of the Western Pacific. Geophysical Monograph, American Geophysical Union, v. 88, p.199-217.

Handley, H.K., Turner, S.P., Smith, I.E., Stewart, R.B. and Cronin, S.J., 2008. Rapid timescales of differentiation and evidence for crustal contamination at intra-oceanic arcs: geochemical and U–Th–Ra–Sr–Nd isotopic constraints from Lopevi Volcano, Vanuatu, SW Pacific. Earth and Planetary Science Letters, v. 273(1-2), p.184-194, https://doi.org/10.1016/j.epsl.2008.06.032

Laporte, C., Cluzel, D., Briqueu, L. and Eissen, J.P., 1998. Isotopic gradient along the New Hebrides arc (Vanuatu, SW Pacific). Collision of the d'Entrecasteaux Zone and heterogeneity of mantle sources. Comptes Rendus de l'Academie des Sciences. Serie 2, Sciences de la Terre et des Planetes, p.101-106.

Lima, S.M., Haase, K.M., Beier, C., Regelous, M., Brandl, P.A., Hauff, F. and Krumm, S., 2017. Magmatic evolution and source variations at the Nifonea Ridge (New Hebrides island arc). Journal of Petrology, v. 58(3), p.473-494, https://doi.org/10.1093/petrology/egx023

Monzier, M., Danyushevsky, L.V., Crawford, A.J., Bellon, H. and Cotten, J., 1993. High-Mg andesites from the southern termination of the New Hebrides island arc (SW Pacific). Journal of Volcanology and Geothermal Research, v. 57(3-4), p. 193-21

Monzier M, Robin C, Eissen JP, Cotten J. 1997. Geochemistry vs. seismo-tectonics along the volcanic New Hebrides central chain (Southwest Pacific). Journal of volcanology and geothermal research, v. 78(1-2), p. 1-29, https://doi.org/10.1016/S0377-0273(97)00006-1

Peate, D.W., Pearce, J.A., Hawkesworth, C.J., Colley, H., Edwards, C.M. and Hirose, K., 1997. Geochemical variations in Vanuatu arc lavas: the role of subducted material and a variable mantle wedge composition. Journal of Petrology, v. 38(10), p.1331-1358, https://doi.org/10.1093/petroj/38.10.1331

Pearce, J.A., Kempton, P.D., and Gill, J.B., 2007. Hf–Nd evidence for the origin and distribution of mantle domains in the SW Pacific, Earth and Planetary Science Letters, v. 260, p. 98-114, https://doi.org/10.1016/j.epsl.2007.05.023

Raos, A.M. and Crawford, A.J., 2004. Basalts from the Efate Island Group, central section of the Vanuatu arc, SW Pacific: geochemistry and petrogenesis. Journal of Volcanology and Geothermal Research, v. 134(1-2), p. 35-56, https://doi.org/10.1016/j.jvolgeores.2003.12.004

Sorbadere, F., Schiano, P., Métrich, N. and Bertagnini, A., 2013. Small-scale coexistence of island-arc-and enriched-MORB-type basalts in the central Vanuatu arc. Contributions to Mineralogy and Petrology, v. 166(5), p. 1305-1321, http://dx.doi.org/10.1007/s00410-013-0928-8

2.2 North Fiji Basin

Eissen, J.P., Lefevre, C., Maillet, P., Morvan, G. and Nohara, M., 1991. Petrology and geochemistry of the central North Fiji Basin spreading centre (Southwest Pacific) between 16 S and 22 S. Marine Geology, v. 98(2-4), p.201-239, https://doi.org/10.1016/0025-3227(91)90104-C

Eissen, J.P., Nohara, M., Cotten, J. and Hirose, K., 1994. North Fiji Basin basalts and their magma sources: Part I. Incompatible element constraints. Marine Geology, v.116(1-2), p.153-178, https://doi.org/10.1016/0025-3227(94)90174-0

Fleutelot, C., Eissen, J.P., Dosso, L., Juteau, T., Launeau, P., Bollinger, C., Cotten, J., Danyushevsky, L. and Savoyant, L., 2005, Petrogenetic variability along the North–South propagating spreading center of the North Fiji Basin ; Mineralogy and Petrology, v. 83, n. 1-2, p.55-86, https://doi.org/10.1007/s00710-004-0061-5

Nohara, M., Hirose, K., Eissen, J.P., Urabe, T. and Joshima, M., 1994. The North Fiji Basin basalts and their magma sources: Part II. Sr-Nd isotopic and trace element constraints, Marine Geology, v. 116(1-2), p. 179-195, https://doi.org/10.1016/0025-3227(94)90175-9

Patriat, M., Falloon, T., Danyushevsky, L., Collot, J., Jean, M.M., Hoernle, K., Hauff, F., Maas, R., Woodhead, J.D. and Feig, S.T., 2019. Subduction initiation terranes exposed at the front of a 2 Ma volcanically-active subduction zone. Earth and Planetary Science Letters, v. 508, p. 30-40, https://doi.org/10.1016/j.epsl.2018.12.011

Pearce, J.A., Kempton, P.D., and Gill, J.B., 2007. Hf–Nd evidence for the origin and distribution of mantle domains in the SW Pacific, Earth and Planetary Science Letters, v. 260, p. 98-114, https://doi.org/10.1016/j.epsl.2007.05.023

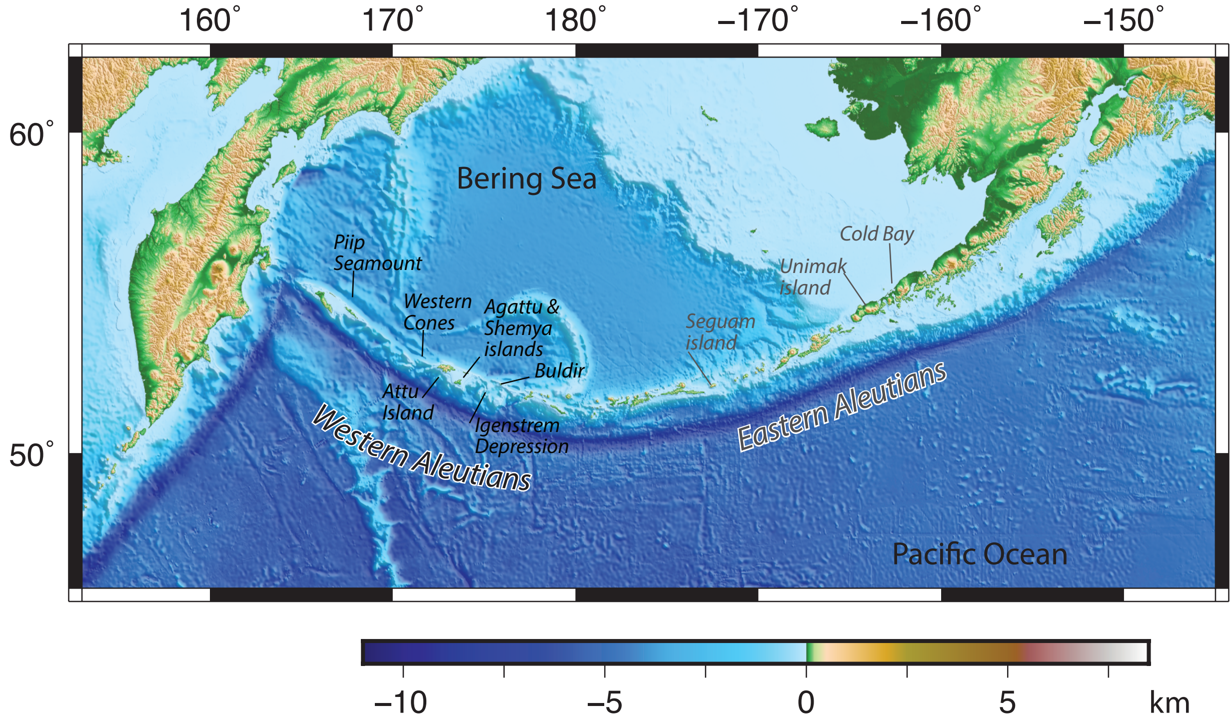

Fig.DR1: Map of the Aleutians subdivided into western Aleutians (black letters) and Eastern Aleutians (gray letters). After Yogodzinski et al., (2015).Bathymetry from Weatherall et al. (2015).

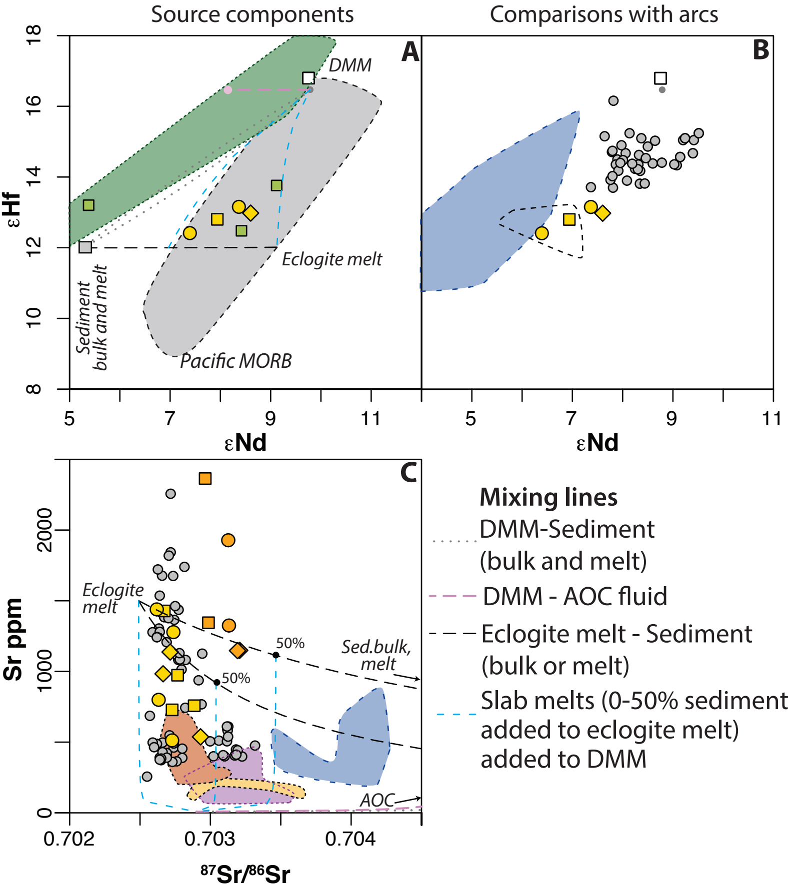

Fig.DR2: A-B) Hf-Nd isotopic composition of Hunter Ridge lavas; **C)** Sr (ppm) as a function of $^{87}Sr/^{86}Sr$ (as in Fig.8 of the main text) with mixing lines added the effect of slab melts onSr abundances and isotopic composition of volcanic rocks. Addition of a slab melt to a DMM leads to strongly variable Sr abundances at unradiogenic $^{87}Sr/^{86}Sr$, whilsts addition of sediment melt or AOC to a DMM leads to a rapid increase in radiogenic $^{87}Sr/^{86}Sr$ at low Sr abundances).Data as in Fig.9 and Table 1 of the main text.

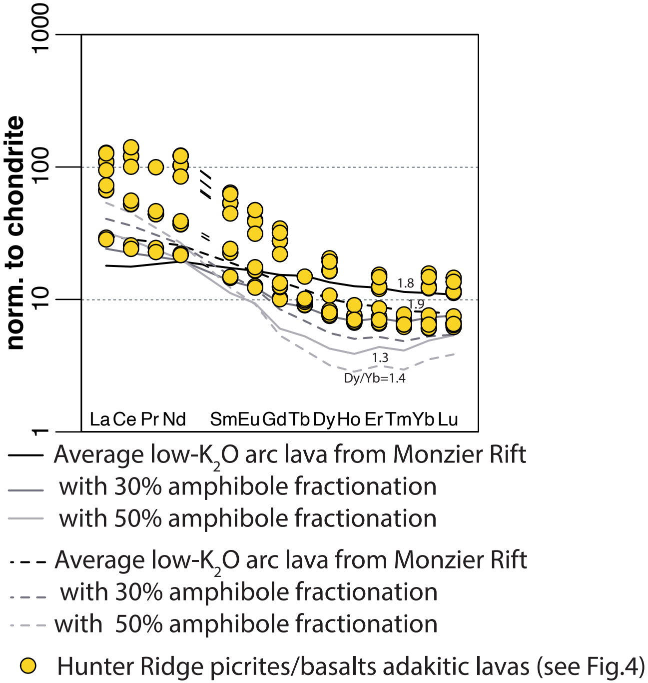

Fig.DR3: This figure illustrates the evolution of REE patterns as a function of amphibole fractionation. Starting compositions are low-K_2O and medium-K_2O arc lavas from the Monzier Rift (data from Patriat et al., 2019). Increments of 30% and 50% amphibole fractionation are shown (assuming constant amphibole-melt Kds of ca. 950°C from Nandekar et al., 2016). Chondrite values are from McDonough and Sun, (1995). Amphibole fractionation will induce trough-like REE patterns, with a decrease in MREE/HREE and only limited increase in LREE/MREE. This is illustrated by the change in Dy/Yb ratio, which gradually diminishes (from 1.9 to 1.3) with increasing amphibole fractionation. Instead, Hunter Ridge and Kadavu adakitic rocks have Gd/Yb (1.5 – 5.7) and Dy/Yb (1.6 – 3.0), whilst also preserving high-Mg# bulk rock compositions.

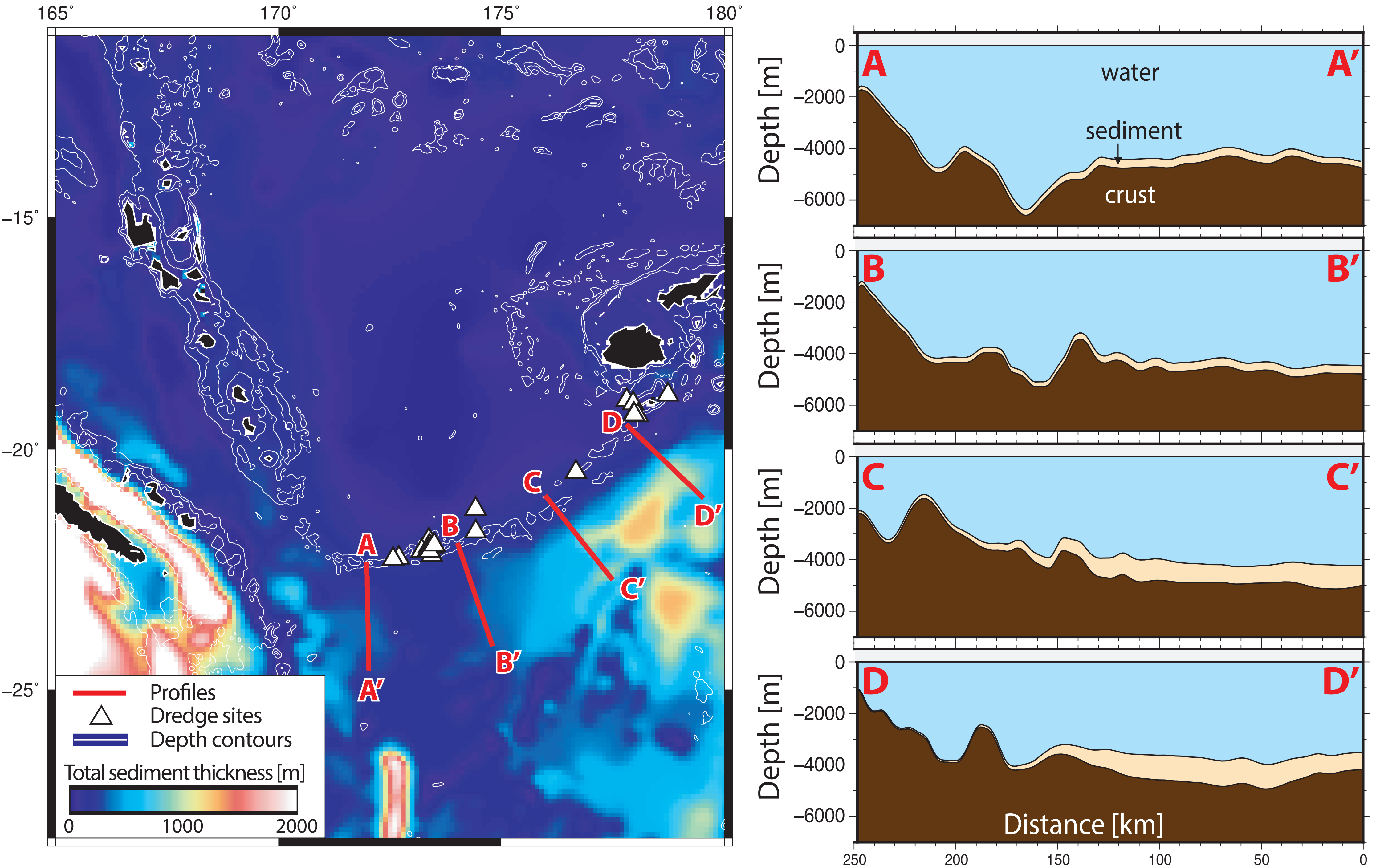

DR4: Estimated thickness of sediments along the South Fiji Basin; total sediment thickness from Straume et al. (2019) and bathymetry from Weatherall et al. (2015).

Year	Voyage	Dredge N°	Sample	Rock type	Geological Setting	Geographical Location	Dredged feature	Lava type	Longitude	Latitude	Water depth (meters)
2006	SS08	D37	D37-1a	glass	Rift	Monzier Rift	Volcanic feature	Andesite	173.393	-22.142	2040
2006	SS08	D37	D37-2	glass	Rift	Monzier Rift	Volcanic feature	Andesite	173.393	-22.142	2040
2006	SS08	D34	D34-1a	glass	Rift	Monzier Rift	Volcanic feature	Basaltic Andesite	173.383	-22.028	1955
2006	SS08	D34	D34-3a	glass	Rift	Monzier Rift	Volcanic feature	Basaltic Andesite	173.383	-22.028	1955
2006	SS08	D36	D36-2	glass	Rift	Monzier Rift	Volcanic feature	Basaltic Andesite	173.374	-22.094	1805
2006	SS08	D36	D36-4	glass	Rift	Monzier Rift	Volcanic feature	Basaltic Andesite	173.374	-22.094	1805
2006	SS08	D36	D36-3	glass	Rift	Monzier Rift	Volcanic feature	Basaltic Andesite	173.374	-22.094	1805
2006	SS08	D37	D37-1a	wholerock	Rift	Monzier Rift	Volcanic feature	Basaltic Andesite	173.393	-22.142	2040
2006	SS08	D37	D37-2	wholerock	Rift	Monzier Rift	Volcanic feature	Basaltic Andesite	173.393	-22.142	2040
2006	SS08	D30	D30-2d	glass	Rift	Monzier Rift	Volcanic feature	Andesite	173.496	-22.011	1872.5
2004	SS10	D15	D15-4	glass	Rift	Monzier Rift	Volcanic feature	Andesite	173.214	-22.130	870
2006	SS08	D30	D30-3d	glass	Rift	Monzier Rift	Volcanic feature	Andesite	173.496	-22.011	1872.5
2006	SS08	D30	D30-11	glass	Rift	Monzier Rift	Volcanic feature	Andesite	173.496	-22.011	1872.5
2006	SS08	D33	D33-2a	glass	Rift	Monzier Rift	Volcanic feature	Basaltic Andesite	173.456	-22.047	1702
2006	SS08	D33	D33-7	glass	Rift	Monzier Rift	Volcanic feature	Basaltic Andesite	173.456	-22.047	1702
2006	SS08	D33	D33-8	glass	Rift	Monzier Rift	Volcanic feature	Basaltic Andesite	173.456	-22.047	1702
2006	SS08	D33	D33-2a	wholerock	Rift	Monzier Rift	Volcanic feature	Picrite	173.456	-22.047	1702
2006	SS08	D33	D33-4	glass	Rift	Monzier Rift	Volcanic feature	Basaltic Andesite	173.456	-22.047	1702
2006	SS08	D33	D33-6	glass	Rift	Monzier Rift	Volcanic feature	Basaltic Andesite	173.456	-22.047	1702
2004	SS10	D22	D22-2	wholerock	Rift	Monzier Rift	Volcanic feature	Andesite	173.493	-22.005	1745
2004	SS10	D22	D22-1	wholerock	Rift	Monzier Rift	Volcanic feature	Andesite	173.493	-22.005	1745
2006	SS08	D30	D30-1d	wholerock	Rift	Monzier Rift	Volcanic feature	Andesite	173.496	-22.011	1872.5
2006	SS08	D30	D30-4a	wholerock	Rift	Monzier Rift	Volcanic feature	Andesite	173.496	-22.011	1872.5
2004	SS10	D15	D15-2	wholerock	Rift	Monzier Rift	Volcanic feature	Basaltic Andesite	173.214	-22.130	870
2006	SS08	D30	D30-9	wholerock	Rift	Monzier Rift	Volcanic feature	Andesite	173.496	-22.011	1872.5
2006	SS08	D30	D30-2e	wholerock	Rift	Monzier Rift	Volcanic feature	Andesite	173.496	-22.011	1872.5
2004	SS10	D15	D15-6	wholerock	Rift	Monzier Rift	Volcanic feature	Basaltic Andesite	173.214	-22.130	870
2006	SS08	D30	D30-5	wholerock	Rift	Monzier Rift	Volcanic feature	Andesite	173.496	-22.011	1872.5
2006	SS08	D30	D30-7b	wholerock	Rift	Monzier Rift	Volcanic feature	Andesite	173.496	-22.011	1872.5
2006	SS08	D30	D30-10	wholerock	Rift	Monzier Rift	Volcanic feature	Andesite	173.496	-22.011	1872.5
2004	SS10	D15	D15-5	wholerock	Rift	Monzier Rift	Volcanic feature	Basaltic Andesite	173.214	-22.130	870
2006	SS08	D30	D30-2d	wholerock	Rift	Monzier Rift	Volcanic feature	Andesite	173.496	-22.011	1872.5
2004	SS10	D15	D15-1	wholerock	Rift	Monzier Rift	Volcanic feature	Basaltic Andesite	173.214	-22.130	870
2004	SS10	D15	D15-3	wholerock	Rift	Monzier Rift	Volcanic feature	Basaltic Andesite	173.214	-22.130	870
2004	SS10	D15	D15-4	wholerock	Rift	Monzier Rift	Volcanic feature	Basaltic Andesite	173.214	-22.130	870
2006	SS08	D30	D30-11	wholerock	Rift	Monzier Rift	Volcanic feature	Basaltic Andesite	173.496	-22.011	1872.5
2006	SS08	D30	D30-3a	wholerock	Rift	Monzier Rift	Volcanic feature	Basaltic Andesite	173.496	-22.011	1872.5
2006	SS08	D33	D33-6	wholerock	Rift	Monzier Rift	Volcanic feature	Picrite	173.456	-22.047	1702
2006	SS08	D33	D33-7	wholerock	Rift	Monzier Rift	Volcanic feature	Picrite	173.456	-22.047	1702
2006	SS08	D30	D30-3d	wholerock	Rift	Monzier Rift	Volcanic feature	Picrite	173.496	-22.011	1872.5
2006	SS08	D33	D33-9	wholerock	Rift	Monzier Rift	Volcanic feature	Picrite	173.456	-22.047	1702
2006	SS08	D33	D33-8	wholerock	Rift	Monzier Rift	Volcanic feature	Picrite	173.456	-22.047	1702
2006	SS08	D19	D19-7	glass	Ridge	Hunter Ridge	Volcanic feature	Basalt	174.420	-21.253	2097.5
2006	SS08	D19	D19-6	glass	Ridge	Hunter Ridge	Volcanic feature	Basalt	174.420	-21.253	2097.5
2006	SS08	D19	D19-3	glass	Ridge	Hunter Ridge	Volcanic feature	Basalt	174.420	-21.253	2097.5
2006	SS08	D19	D19-8	glass	Ridge	Hunter Ridge	Volcanic feature	Basalt	174.420	-21.253	2097.5
2006	SS08	D19	D19-1	glass	Ridge	Hunter Ridge	Volcanic feature	Basalt	174.420	-21.253	2097.5
2004	SS10	D27A	D27A-1	glass	Ridge	Hunter Ridge	Top of escarpment	Basaltic Andesite	173.372	-21.904	1685
2004	SS10	D27A	D27A-3a	wholerock	Ridge	Hunter Ridge	Top of escarpment	Picrite	173.372	-21.904	1685
2004	SS10	D27A	D27A-6a	wholerock	Ridge	Hunter Ridge	Top of escarpment	Picrite	173.372	-21.904	1685
2009	SS03	D71	D71-3	wholerock	Incipient Rift	Hunter Ridge	Volcanic feature	Picrite	172.699	-22.279	1860
2009	SS03	D71	D71-1	wholerock	Incipient Rift	Hunter Ridge	Volcanic feature	Picrite	172.699	-22.279	1860
2004	SS10	D27A	D27A-1	wholerock	Ridge	Hunter Ridge	Top of escarpment	Basalt	173.372	-21.904	1685
2009	SS03	D71	D71-9	wholerock	Incipient Rift	Hunter Ridge	Volcanic feature	Picrite	172.699	-22.279	1860
2009	SS03	D64	D64-3	wholerock	Ridge	Hunter Ridge	Volcanic feature	Basaltic Andesite	173.437	-22.222	1475
2009	SS03	D55	D55-4a	wholerock	Ridge	Hunter Ridge	Volcanic feature	Andesite	176.670	-20.476	1635
2006	SS08	D17	D17-9	wholerock	Ridge	Hunter Ridge	Volcanic feature	Andesite	174.423	-21.730	1310
2004	SS10	D17	D24-2	wholerock	Ridge	Hunter Ridge	Volcanic feature	Andesite	174.397	-21.817	1675
2009	SS03	D74	D74-4	wholerock	Incipient Rift	Hunter Ridge	Volcanic feature	Andesite	172.569	-22.304	1003
2009	SS03	D74	D74-6	wholerock	Incipient Rift	Hunter Ridge	Volcanic feature	Andesite	172.569	-22.304	1003
2006	SS08	D17	D17-7	wholerock	Ridge	Hunter Ridge	Volcanic feature	Andesite	174.423	-21.730	1310
2004	SS10	D17	D24-3	wholerock	Ridge	Hunter Ridge	Volcanic feature	Andesite	174.397	-21.817	1675
2006	SS08	D10	D10-4	wholerock	NE tip of Hunter Ridge	Kadavu	Volcanic feature	Basalt	177.995	-19.257	685
2006	SS08	D10	D10-2	wholerock	NE tip of Hunter Ridge	Kadavu	Volcanic feature	Basalt	177.995	-19.257	685
2006	SS08	D2	D2-2a	wholerock	NE tip of Hunter Ridge	Kadavu	Volcanic feature	Basalt	177.807	-18.950	1840
2006	SS08	D2	D2-3a	wholerock	NE tip of Hunter Ridge	Kadavu	Volcanic feature	Basalt	177.807	-18.950	1840
2006	SS08	D2	D2-4	glass	NE tip of Hunter Ridge	Kadavu	Volcanic feature	Basaltic Andesite	177.807	-18.950	1840
2006	SS08	D2	D2-3	glass	NE tip of Hunter Ridge	Kadavu	Volcanic feature	Basaltic Andesite	177.807	-18.950	1840
2006	SS08	D10	D10-1	wholerock	NE tip of Hunter Ridge	Kadavu	Volcanic feature	Basaltic Andesite	177.995	-19.257	685
2006	SS08	D4	D4-2	wholerock	NE tip of Hunter Ridge	Kadavu	Volcanic feature	Basaltic Andesite	177.951	-19.022	1455
2006	SS08	D4	D4-5	wholerock	NE tip of Hunter Ridge	Kadavu	Volcanic feature	Basaltic Andesite	177.951	-19.022	1455
2006	SS08	D4	D4-7	wholerock	NE tip of Hunter Ridge	Kadavu	Volcanic feature	Basaltic Andesite	177.951	-19.022	1455
2006	SS08	D4	D4-3a	wholerock	NE tip of Hunter Ridge	Kadavu	Volcanic feature	Basaltic Andesite	177.951	-19.022	1455
2006	SS08	D4	D4-3	wholerock	NE tip of Hunter Ridge	Kadavu	Volcanic feature	Basaltic Andesite	177.951	-19.022	1455
2006	SS08	D4	D4-6	wholerock	NE tip of Hunter Ridge	Kadavu	Volcanic feature	Basaltic Andesite	177.951	-19.022	1455
2006	SS08	D4	D4-4	wholerock	NE tip of Hunter Ridge	Kadavu	Volcanic feature	Basaltic Andesite	177.951	-19.022	1455
2006	SS08	D12	D12-8	wholerock	NE tip of Hunter Ridge	Kadavu	Volcanic feature	Basaltic Andesite	178.060	-19.277	1340
2006	SS08	D12	D12-5	wholerock	NE tip of Hunter Ridge	Kadavu	Volcanic feature	Basaltic Andesite	178.060	-19.277	1340
2006	SS08	D5	D5-7	wholerock	NE tip of Hunter Ridge	Kadavu	Volcanic feature	Basaltic Andesite	178.734	-18.833	1157.5
2006	SS08	D4	D4-3a	glass	NE tip of Hunter Ridge	Kadavu	Volcanic feature	Andesite	177.951	-19.022	1455
2006	SS08	D4	D4-3b	glass	NE tip of Hunter Ridge	Kadavu	Volcanic feature	Andesite	177.951	-19.022	1455
2006	SS08	D8	D8-3	wholerock	NE tip of Hunter Ridge	Kadavu	Volcanic feature	Andesite	177.964	-19.250	892.5
2006	SS08	D9	D9-2	wholerock	NE tip of Hunter Ridge	Kadavu	Escarpment	Andesite	177.975	-19.255	665

DR5 Table 1:Characteristics of dredged samples used for this study. Samples vary from fresh to slightly altered sparsely phyric massive flows to highly olivine phyric lava flows and finally to quenched pillow margins with preserved volcanic glass. Although phenocryst abundances vary significantly from one sample to another, they are typically dominated by mm-sized olivine containing spinel inclusions, as well as clinopyroxene and plagioclase phenocrysts. Orthopyroxene phenocrysts are also present in high-Mg# adakites, whilst amphibole remains rather sparse. See Patriat et al., 2019 (supplementary appendix) for images of dredged rocks and thin section images of highly vesicular adakitic rock and sparsely phyric, fine-grained back-arc basalt from Hunter Ridge and Monzier Rift. Description of high-Mg adakitic rocks from Kadavu can be found in Danyushevsky et al., (2008) (supplementary appendix)

Sample	Rock type	Geographical Location	SiO_2	TiO_2	Al_2O_3	FeO_T	MnO	MgO	CaO	Na_2O	K_2O	P_2O_5	Cr_2O_3	NiO	LOI	Total	$Mg\#_{Fetot}$
D37-1a	glass	Monzier Rift	62.47	0.95	14.83	8.42	0.14	2.47	5.80	3.81	0.93	0.18	0.00			100.00	34.36
D37-2	glass	Monzier Rift	62.09	0.95	14.96	8.40	0.14	2.62	5.89	3.83	0.92	0.19	0.01			100.00	35.69
D34-1a	glass	Monzier Rift	55.63	1.09	16.12	8.84	0.17	4.22	8.11	3.51	1.88	0.42	0.00			100.00	45.99
D34-3a	glass	Monzier Rift	55.52	1.10	16.13	8.87	0.18	4.28	8.05	3.58	1.88	0.42	0.00			100.00	46.22
D36-2	glass	Monzier Rift	55.52	0.72	16.13	8.09	0.15	5.18	9.39	3.59	0.94	0.27	0.00			100.00	53.30
D36-4	glass	Monzier Rift	55.41	0.70	16.13	7.98	0.15	5.30	9.57	3.55	0.92	0.27	0.01			100.00	54.24
D36-3	glass	Monzier Rift	55.56	0.69	16.31	7.93	0.15	5.28	9.35	3.54	0.91	0.27	0.01			100.00	54.27
D37-1a	wholerock	Monzier Rift	56.87	0.54	17.70	6.81	0.11	4.67	8.76	3.67	0.75	0.12			1.29	99.73	54.99
D37-2	wholerock	Monzier Rift	56.84	0.54	17.57	6.87	0.11	4.83	8.79	3.77	0.55	0.12			0.96	99.81	55.62
D30-2d	glass	Monzier Rift	62.54	0.72	16.98	5.17	0.08	3.68	5.85	3.22	1.50	0.27	0.01			100.00	55.94
D15-4	glass	Monzier Rift	57.96	0.54	15.69	6.80	0.12	5.17	9.07	3.07	1.32	0.24	0.01			100.00	57.51
D30-3d	glass	Monzier Rift	57.41	0.69	16.68	6.55	0.12	5.10	8.68	3.59	0.95	0.23	0.01			100.00	58.11
D30-11	glass	Monzier Rift	58.80	0.69	16.98	5.71	0.10	4.62	8.03	3.47	1.28	0.32	0.01			100.00	59.04
D33-2a	glass	Monzier Rift	52.74	0.65	15.82	7.91	0.16	7.18	12.66	2.30	0.40	0.17	0.02			100.00	61.82
D33-7	glass	Monzier Rift	52.99	0.64	15.52	7.80	0.14	7.16	12.75	2.42	0.40	0.16	0.01			100.00	62.08
D33-8	glass	Monzier Rift	52.98	0.64	15.51	7.77	0.15	7.16	12.73	2.47	0.40	0.16	0.02			100.00	62.16
D33-2a	wholerock	Monzier Rift	52.88	0.95	17.14	7.09	0.13	6.70	11.14	3.53	0.31	0.10	0.02	0.00	0.58	100.45	62.74
D33-4	glass	Monzier Rift	52.78	0.64	15.49	7.73	0.15	7.34	12.88	2.43	0.39	0.16	0.03			100.00	62.87
D33-6	glass	Monzier Rift	52.63	0.65	15.33	7.71	0.15	7.51	13.04	2.40	0.38	0.17	0.03			100.00	63.45
D22-2	wholerock	Monzier Rift	61.08	0.41	14.54	4.97	0.09	7.37	6.27	4.20	0.90	0.17			0.77	100.08	72.53
D22-1	wholerock	Monzier Rift	61.04	0.41	14.63	4.95	0.09	7.34	6.30	4.16	0.92	0.16			0.87	100.04	72.53
D30-1d	wholerock	Monzier Rift	61.32	0.39	14.52	4.95	0.09	7.33	6.16	4.14	0.90	0.16	0.03	0.01	1.02	99.82	72.54
D30-4a	wholerock	Monzier Rift	61.29	0.38	14.57	4.92	0.09	7.37	6.17	4.13	0.89	0.16	0.03	0.01	0.76	100.09	72.74
D15-2	wholerock	Monzier Rift	54.75	0.48	12.65	7.53	0.14	11.32	9.42	2.43	0.98	0.20	0.09	0.02		99.57	72.82
D30-9	wholerock	Monzier Rift	61.13	0.39	14.45	4.93	0.09	7.62	6.12	4.13	0.92	0.17	0.03	0.01	0.85	99.71	73.34
D30-2e	wholerock	Monzier Rift	58.98	0.48	14.53	5.18	0.09	8.33	6.76	4.13	1.26	0.20	0.04	0.01	1.86	100.17	74.12
D15-6	wholerock	Monzier Rift	54.30	0.46	12.19	7.56	0.14	12.17	9.30	2.62	0.95	0.20	0.09	0.02		98.91	74.14
D30-5	wholerock	Monzier Rift	60.88	0.38	14.28	4.95	0.09	7.97	6.25	3.97	1.02	0.15	0.03	0.01	1.51	100.35	74.15
D30-7b	wholerock	Monzier Rift	60.95	0.37	14.13	5.04	0.09	8.18	6.17	4.03	0.85	0.15	0.04	0.01	0.84	100.04	74.31
D30-10	wholerock	Monzier Rift	60.96	0.38	14.16	5.03	0.09	8.17	6.17	3.99	0.86	0.15	0.04	0.01	0.83	99.87	74.33

DR6 Table 2: Major element composition of bulk rocks (XRF analysis) or glass (Microprobe) of dredged samples

Sample	Rock type	Geographical Location	SiO_2	TiO_2	Al_2O_3	FeO_T	MnO	MgO	CaO	Na_2O	K_2O	P_2O_5	Cr_2O_3	NiO	LOI	Total	$Mg\#_{Fetot}$
D15-5	wholerock	Monzier Rift	54.39	0.45	12.00	7.53	0.13	12.34	9.43	2.52	0.90	0.19	0.10	0.03		98.80	74.49
D30-2d	wholerock	Monzier Rift	58.36	0.51	14.45	5.31	0.09	8.78	6.98	4.10	1.16	0.21	0.04	0.02	1.58	99.69	74.67
D15-1	wholerock	Monzier Rift	54.35	0.43	11.53	7.22	0.13	13.17	9.39	2.35	1.09	0.20	0.12	0.03		98.91	76.48
D15-3	wholerock	Monzier Rift	54.23	0.43	11.58	7.21	0.13	13.18	9.47	2.38	1.06	0.19	0.11	0.03		99.36	76.50
D15-4	wholerock	Monzier Rift	54.69	0.43	12.07	6.99	0.12	12.84	9.14	2.59	0.97	0.17			1.04	99.65	76.60
D30-11	wholerock	Monzier Rift	55.08	0.51	13.20	6.21	0.11	12.01	8.06	3.34	1.08	0.27	0.08	0.04	1.34	99.93	77.51
D30-3a	wholerock	Monzier Rift	54.84	0.51	13.13	6.22	0.11	12.12	8.22	3.32	1.15	0.28	0.08	0.04	1.60	99.87	77.65
D33-6	wholerock	Monzier Rift	49.67	0.47	11.64	8.06	0.15	17.02	10.25	2.04	0.29	0.14	0.22	0.06	0.34	99.76	79.01
D33-7	wholerock	Monzier Rift	49.30	0.44	11.10	8.11	0.15	18.44	9.81	1.94	0.28	0.13	0.23	0.06	0.43	99.82	80.21
D30-3d	wholerock	Monzier Rift	52.71	0.43	11.79	6.87	0.12	15.80	8.61	2.65	0.67	0.15	0.14	0.06	0.87	99.60	80.39
D33-9	wholerock	Monzier Rift	48.94	0.46	10.90	8.15	0.15	18.75	10.13	1.83	0.27	0.12	0.24	0.06	0.14	99.88	80.39
D33-8	wholerock	Monzier Rift	49.00	0.44	10.92	8.19	0.15	18.93	9.67	1.96	0.31	0.13	0.23	0.06	0.77	100.21	80.46
D19-7	glass	Hunter Ridge	50.46	0.84	16.13	8.74	0.17	7.39	13.17	2.12	0.68	0.30	0.01			100.00	60.12
D19-6	glass	Hunter Ridge	50.60	0.84	16.14	8.77	0.17	7.33	13.07	2.10	0.68	0.31	0.00			100.00	59.84
D19-3	glass	Hunter Ridge	50.68	0.82	16.03	8.72	0.17	7.33	13.10	2.15	0.68	0.32	0.01			100.00	59.97
D19-8	glass	Hunter Ridge	50.73	0.81	16.07	8.78	0.19	7.27	12.94	2.20	0.68	0.32	0.01			100.00	59.60
D19-1	glass	Hunter Ridge	50.74	0.80	16.22	8.59	0.16	7.38	12.98	2.14	0.66	0.31	0.02			100.00	60.47
D27A-1	glass	Hunter Ridge	55.58	0.67	15.91	8.15	0.15	5.48	9.60	3.07	1.02	0.37	0.00			100.00	54.52
D27A-3a	wholerock	Hunter Ridge	50.78	0.46	11.29	8.84	0.15	15.72	9.69	2.11	0.70	0.25			0.97	99.66	76.01
D27A-6a	wholerock	Hunter Ridge	51.71	0.47	11.60	7.92	0.15	15.06	9.89	2.16	0.79	0.25			0.74	100.14	77.22
D71-3	wholerock	Hunter Ridge	51.80	0.37	10.59	8.50	0.16	16.82	8.85	1.69	1.06	0.172			0.44	99.58	77.91
D71-1	wholerock	Hunter Ridge	51.84	0.38	10.89	8.47	0.16	16.43	8.84	1.75	1.07	0.172			0.42	99.95	77.56
D27A-1	wholerock	Hunter Ridge	52.18	0.48	11.99	7.77	0.14	13.92	10.17	2.32	0.76	0.26			1.13	99.69	76.14
D71-9	wholerock	Hunter Ridge	52.54	0.39	10.90	8.33	0.16	15.13	9.41	1.90	1.06	0.171			0.68	99.76	76.39
D64-3	wholerock	Hunter Ridge	56.03	0.50	15.61	6.69	0.12	6.98	9.50	2.52	1.57	0.426	0.034	0.010	2.21	99.77	65.02
D55-4a	wholerock	Hunter Ridge	59.22	0.46	14.17	5.73	0.10	7.09	7.82	2.68	2.31	0.358	0.038	0.012	2.20	99.81	68.77
D17-9	wholerock	Hunter Ridge	61.05	0.50	15.94	5.59	0.10	4.64	7.11	3.78	1.08	0.19			1.01	99.44	59.65
D24-2	wholerock	Hunter Ridge	61.30	0.38	15.96	4.69	0.08	5.91	6.29	4.24	0.97	0.14	0.02	0.02		99.13	69.18
D74-4	wholerock	Hunter Ridge	61.33	0.39	15.20	5.87	0.11	5.06	7.23	3.54	1.11	0.125	0.021	0.004	0.87	100.07	60.58
D74-6	wholerock	Hunter Ridge	61.44	0.40	15.22	5.80	0.11	5.00	7.21	3.53	1.14	0.125	0.020	0.004	1.07	99.95	60.57

DR6 Table 2: continued

Sample	Rock type	Geographical Location	SiO_2	TiO_2	Al_2O_3	FeO_T	MnO	MgO	CaO	Na_2O	K_2O	P_2O_5	Cr_2O_3	NiO	LOI	Total	$Mg\#_{Fetot}$
D17-7	wholerock	Hunter Ridge	61.48	0.49	16.04	5.47	0.10	4.35	6.90	3.81	1.17	0.19			1.25	99.63	58.62
D24-3	wholerock	Hunter Ridge	62.39	0.33	15.10	4.22	0.07	6.64	5.73	4.57	0.81	0.12			2.65	100.07	73.70
D10-4	wholerock	Kadavu	48.61	1.06	17.07	7.04	0.13	11.12	9.96	3.55	0.81	0.64			3.15	99.74	73.78
D10-2	wholerock	Kadavu	49.56	1.10	17.03	6.94	0.12	9.89	10.24	3.79	0.69	0.62			2.00	99.58	71.75
D2-2a	wholerock	Kadavu	50.28	1.26	15.61	6.97	0.12	10.44	10.12	3.35	1.23	0.63			0.78	100.15	72.73
D2-3a	wholerock	Kadavu	50.36	1.28	15.54	6.94	0.12	10.66	9.77	3.44	1.25	0.65			0.71	100.17	73.24
D2-4	glass	Kadavu	52.19	1.79	16.51	7.32	0.14	5.92	10.58	3.36	1.43	0.76	0.01			100.00	59.04
D2-3	glass	Kadavu	52.39	1.74	16.66	7.26	0.14	5.74	10.37	3.44	1.48	0.77	0.01			100.00	58.48
D10-1	wholerock	Kadavu	52.72	1.02	16.66	6.33	0.11	8.73	9.26	3.47	1.26	0.45			1.13	100.13	71.09
D4-2	wholerock	Kadavu	54.02	1.26	16.34	6.22	0.11	7.03	8.68	4.10	1.70	0.55			0.87	99.40	66.83
D4-5	wholerock	Kadavu	54.05	1.27	16.28	6.20	0.10	7.08	8.74	4.05	1.68	0.54			0.93	99.56	67.06
D4-7	wholerock	Kadavu	54.12	1.28	16.34	6.18	0.11	7.05	8.56	4.10	1.72	0.54			0.85	100.12	67.03
D4-3a	wholerock	Kadavu	54.14	1.27	16.30	6.20	0.10	7.08	8.68	4.05	1.65	0.52			1.11	99.71	67.03
D4-3	wholerock	Kadavu	54.18	1.25	16.37	6.16	0.10	7.01	8.63	4.07	1.68	0.54			0.94	99.73	66.97
D4-6	wholerock	Kadavu	55.41	1.16	16.24	5.80	0.10	6.66	8.33	4.18	1.63	0.50			0.53	100.07	67.20
D4-4	wholerock	Kadavu	55.96	1.16	16.21	5.74	0.10	6.18	8.15	4.09	1.90	0.50			1.28	99.67	65.71
D12-8	wholerock	Kadavu	56.04	1.16	15.88	5.10	0.08	6.51	8.56	4.26	1.80	0.60			1.09	99.62	69.48
D12-5	wholerock	Kadavu	56.36	1.13	15.81	5.04	0.08	6.54	8.48	4.19	1.78	0.58			1.45	99.81	69.81
D5-7	wholerock	Kadavu	56.74	0.77	19.66	5.30	0.07	1.79	5.80	4.28	4.97	0.60			1.20	99.89	37.61
D4-3a	glass	Kadavu	57.44	2.06	16.17	7.29	0.12	3.63	6.32	3.78	2.37	0.82	0.00			100.00	47.04
D4-3b	glass	Kadavu	57.77	2.04	16.21	7.30	0.14	3.60	6.36	3.42	2.32	0.84	0.00			100.00	46.78
D8-3	wholerock	Kadavu	58.25	0.59	14.61	6.02	0.11	7.05	7.81	3.17	2.06	0.33			1.39	99.81	67.60
D9-2	wholerock	Kadavu	58.85	0.58	14.60	5.89	0.11	6.61	7.66	3.26	2.13	0.32			1.23	100.12	66.65

DR6 Table 2: continued

Sample	D37-1a	D37-2	D34-1a	D34-3a	D36-2	D36-4	D36-3	D37-1a	D37-2	D30-2d	D15-4	D30-3d	D30-11
XRF													
Y								10.8	10.4				
Rb								7.9	5.9				
Zn								52	53				
Cu								68	85				
Ni								21	23				
Sr								616	609				
Zr								68	67				
Cr								54	61				
Ba								98	98				
V								252	253				
La								4	5				
Ce								14	13				
Nd								10	9				
Sc								25	24				
ICPMS													
Li	3.96	3.34	4.98	6.27	4.68	4.83	4.70	2.97	3.44	7.24	5.51	4.66	6.73
Be	0.54	0.50	0.96	1.15	0.71	0.68	0.70	0.60	0.57	0.74	0.99	0.54	0.84
B	11.65	10.19	12.39	18.74	15.44	14.60	13.78			15.53		11.22	17.50
Sc	19.70	14.14	16.49	19.54	24.02	22.98	20.23	27.63	23.45	12.70	25.18	19.65	19.88
V	288	188	260	308	221	240	232	253	223	165	212	181	194
Cr	9.8	4.8	0.6	0.7	27.5	4.1	1.8	71.9	48.7	21.1	62.8	106.5	55.5
Co	18.13	12.38	17.86	20.89	24.44	26.32	28.63	27.33	25.50	14.73	25.81	21.40	17.46
Ni	8.31	5.58	5.22	6.37	24.64	23.59	42.25	26.10	25.26	23.43	33.86	30.13	32.26
Cu	75.59	63.33	74.19	87.32	67.39	74.17	72.22	68.67	77.26	42.90	118.24	82.03	48.90
Zn	55.35	40.97	57.37	66.08	58.40	64.65	66.53	53.23	49.84	48.65	51.54	45.77	53.10
Rb	5.98	4.86	25.49	28.36	7.58	8.58	8.46	7.97	5.49	14.55	13.31	9.24	13.17
Sr	499	542	1005	886	865	953	973	662	643	1606	1021	1275	1957
Y	10.33	8.30	15.25	16.66	11.54	12.82	11.54	10.91	10.38	8.10	12.32	9.51	10.48
Zr	59.44	47.76	83.58	91.31	78.77	88.67	82.35	67.73	63.71	101.21	84.18	76.71	98.62
Nb	0.58	0.47	1.86	2.05	0.83	0.95	0.93	0.59	0.54	1.10	2.04	0.81	1.22
Mo								0.31	0.23				
Cs	0.06	0.05	0.17	0.19	0.06	0.07	0.07	0.06	0.06	0.18	0.18	0.10	0.11
Ba	103	88	212	221	127	145	144	100	104	300	346	205	328
La	6.00	4.92	19.77	21.16	15.13	17.37	16.63	5.97	5.62	14.58	26.23	10.60	25.78
Ce	14.61	12.12	44.23	47.83	35.13	40.43	39.61	15.14	13.66	33.32	56.95	25.67	58.63
Pr								2.20	2.01				
Nd	9.57	7.88	25.77	27.40	21.58	24.45	23.27	10.14	9.39	19.33	27.00	15.24	32.99
Sm	2.22	1.82	5.38	5.73	3.98	4.61	4.25	2.42	2.23	3.46	5.05	2.97	5.32
Eu	0.76	0.62	1.64	1.71	1.18	1.30	1.27	0.80	0.75	1.02	1.49	0.91	1.50
Gd	2.14	1.72	4.34	4.54	2.95	3.45	3.12	2.38	2.26	2.37	3.82	2.28	3.43
Tb								0.37	0.35				
Dy	2.09	1.64	3.29	3.45	2.32	2.63	2.50	2.10	2.02	1.68	2.50	1.78	2.26
Ho								0.40	0.40				
Er	1.14	0.90	1.62	1.66	1.20	1.37	1.23	1.18	1.15	0.83	1.26	1.02	1.06
Tm								0.17	0.17				
Yb	1.23	0.98	1.61	1.62	1.25	1.41	1.35	1.10	1.08	0.83	1.15	0.99	1.07
Lu	0.17	0.14	0.22	0.24	0.19	0.21	0.19	0.17	0.17	0.12	0.17	0.16	0.15
Hf	1.75	1.41	2.28	2.34	2.05	2.33	2.19	1.84	1.84	2.61	2.16	2.06	2.59
Ta	0.04	0.03	0.11	0.11	0.05	0.06	0.06	0.04	0.04	0.07	0.11	0.05	0.08
W								0.12	0.05				
Pb	1.57	1.32	2.88	2.95	1.99	2.33	2.33	1.28	1.32	4.17	3.92	2.11	3.96
Th	0.76	0.62	2.13	2.16	1.61	1.91	1.80	0.75	0.67	1.80	3.79	1.53	3.04
U	0.30	0.26	1.02	1.02	0.51	0.59	0.60	0.26	0.25	0.61	1.30	0.45	0.87

DR7 Table 3: Trace element analysis of bulk rocks and glass of dredged samples

Sample	D33-2a	D33-7	D33-8	D33-2a	D33-4	D33-6	D22-2	D22-1	D30-1d	D30-4a	D15-2	D30-9	D30-2e
XRF													
Y				20.2			6.0	5.3	6.2	5.6	10.0	5.7	6.5
Rb				2.8			10.9	11.7	10.5	10.8	10.7	10.9	13.3
Zn				60			45	44	47	45	65	44	47
Cu				44			45	44	45	44	84	41	45
Ni				30			74	66	69	74	174	77	102
Sr				237			1175	1185	1127	1146	809	1147	1423
Zr				66			91	94	89	92	67	92	94
Cr				157			235	222	220	227	576	230	249
Ba				44			227	211	214	215	232	217	250
V				204			116	110	110	111	193	112	124
La				<2			8	7	6	9	16	6	8
Ce				9					24	23	40	19	29
Nd				9					14	14	20	13	19
Sc				33					15	15	30	14	16
ICPMS													
Li	4.79	4.90	4.78		4.88	4.74	5.70	5.32		5.69	3.44	5.96	3.10
Be	0.33	0.32	0.41		0.33	0.37	0.83	0.80		0.64	0.70	0.66	0.65
B	18.52	16.37	19.48		17.29	17.11							
Sc	43.09	41.43	43.93		44.64	47.06	17.30	17.21		14.70	31.30	14.76	14.70
V	287	287	281		286	284	123	123		109	188	109	114
Cr	161.0	145.9	185.7		195.0	286.9	249.6	244.5		229.0	580.0	235.1	267.0
Co	32.62	32.87	32.30		32.46	32.66	25.96	25.55		25.30	44.31	26.54	28.17
Ni	47.20	46.22	47.84		48.11	46.10	85.89	84.42		85.00	187.00	91.04	114.00
Cu	72.53	69.46	68.99		68.05	67.48	47.84	46.53		43.00	89.00	40.90	42.00
Zn	66.12	64.11	63.79		71.04	63.21	43.93	43.08		45.00	60.00	46.17	46.00
Rb	3.55	3.72	3.62		3.68	3.52	10.74	10.64		9.75	10.60	10.01	11.80
Sr	736	739	728		733	718	1137	1115		1027	792	1046	1289
Y	14.19	13.26	13.67		13.99	13.83	6.19	6.21		6.04	11.00	6.18	7.07
Zr	50.29	47.92	49.67		50.61	49.19	90.02	90.36		86.50	64.70	88.67	91.80
Nb	0.76	0.77	0.76		0.77	0.76	0.78	0.80		0.77	1.78	0.76	0.93
Mo										0.48	0.71	0.46	0.55
Cs	0.04	0.04	0.04		0.04	0.04	0.16	0.15		0.14	0.12	0.14	0.14
Ba	80	84	82		83	81	224	223		213	238	219	244
La	9.80	9.70	9.72		9.90	9.70	9.54	9.53		8.97	17.80	9.22	11.30
Ce	22.55	22.78	22.59		23.00	22.28	21.42	21.71		20.20	36.00	20.79	25.50
Pr							2.99	3.00		2.76	4.58	2.85	3.54
Nd	14.28	14.07	14.33		14.22	14.04	12.21	12.33		11.90	18.50	12.19	15.50
Sm	3.03	2.79	2.93		2.99	2.94	2.37	2.38		2.32	3.55	2.36	2.94
Eu	0.92	0.91	0.90		0.93	0.92	0.72	0.75		0.72	1.05	0.76	0.91
Gd	2.68	2.45	2.57		2.63	2.64	1.72	1.75		1.71	2.83	1.73	2.07
Tb							0.22	0.23		0.23	0.40	0.23	0.28
Dy	2.75	2.54	2.62		2.66	2.69	1.22	1.22		1.21	2.18	1.24	1.42
Ho							0.23	0.23		0.23	0.43	0.23	0.27
Er	1.56	1.43	1.48		1.50	1.52	0.63	0.66		0.62	1.16	0.65	0.74
Tm							0.09	0.09		0.09	0.16	0.09	0.11
Yb	1.68	1.53	1.60		1.61	1.63	0.61	0.60		0.58	1.05	0.60	0.64
Lu	0.24	0.22	0.23		0.24	0.24	0.09	0.09		0.08	0.16	0.09	0.10
Hf	1.49	1.37	1.45		1.46	1.45	2.20	2.20		2.13	1.70	2.20	2.24
Ta	0.04	0.04	0.04		0.04	0.04	0.05	0.06		0.05	0.10	0.06	0.06
W										0.21	0.33	0.14	0.22
Pb	2.47	1.46	1.62		1.87	1.43	2.63	2.62		2.55	3.09	2.63	2.84
Th	0.95	0.92	0.96		0.96	0.93	1.33	1.33		1.21	2.55	1.26	1.35
U	0.30	0.31	0.31		0.31	0.30	0.46	0.45		0.44	0.96	0.46	0.48

DR7 Table 3: continued

Sample	D15-6	D30-5	D30-7b	D30-10	D15-5	D30-2d	D15-1	D15-3	D15-4	D30-11	D30-3a	D33-6	D33-7
XRF													
Y	10.3	5.3	5.2	5.5	10.1	7.2	10.9	10.7	10.7	9.4	8.9	10.9	10.2
Rb	11.1	11.8	10	9.9	10.2	12.3	11.1	11.3	10.6	11.2	11.8	3.1	2.7
Zn	61	43	45	45	56	50	60	59	57	57	56	62	62
Cu	82	42	42	42	70	44	76	74	69	53	52	62	63
Ni	191	73	87	83	196	118	250	238	226	281	278	439	484
Sr	754	1120	1111	1099	746	1464	803	810	760	1543	1527	535	513
Zr	62	86	87	86	63	93	69	70	69	94	93	45	43
Cr	609	234	280	253	648	272	774	767	710	534	527	1467	1520
Ba	224	209	201	199	226	254	301	304	245	270	265	66	64
V	192	109	107	107	195	128	187	187	171	150	152	212	201
La	17	7	7	5	16	11	21	23	21	18	18	9	7
Ce	36	22	23	20	34	30	56	52		50	55	20	17
Nd	19	11	12	13	20	18	28	28		29	28	12	12
Sc	31	15	16	15	30	17	28	28		19	19	31	30
ICPMS													
Li	3.16	4.29	5.55	5.68	3.36	3.69	3.93	3.84	4.65		3.22		
Be	0.63	0.62	0.60	0.64	0.65	0.64	0.71	0.70	0.93		0.62		
B													
Sc	30.60	15.30	14.90	14.98	32.90	15.10	30.40	29.70	27.56		18.50		
V	133	106	107	107	183	119	174	176	182		140		
Cr	635.0	249.0	273.0	262.6	702.0	273.0	757.0	752.0	493.0		513.0		
Co	46.23	26.39	27.13	28.13	45.46	28.33	46.02	46.96	42.54		39.48		
Ni	209.00	91.00	101.00	101.70	212.00	128.00	250.00	254.00	228.32		294.00		
Cu	83.00	42.00	42.00	42.54	67.00	41.00	74.00	75.00	71.10		48.00		
Zn	60.00	45.00	45.00	45.87	55.00	49.00	58.00	58.00	57.58		56.00		
Rb	9.81	10.70	8.98	9.15	10.00	11.20	11.30	10.50	10.38		9.77		
Sr	715	1044	991	983	734	1371	803	788	758		1428		
Y	10.30	5.89	5.86	5.86	10.60	7.37	11.40	11.10	10.49		8.73		
Zr	61.20	83.00	83.50	83.05	60.80	90.80	68.60	67.40	67.94		88.20		
Nb	1.70	0.72	0.73	0.73	1.69	0.88	1.79	1.79	1.56		0.99		
Mo	0.65	0.45	0.44	0.46	0.69	0.54	0.69	0.69	0.70		0.53		
Cs	0.10	0.14	0.12	0.13	0.11	0.13	0.15	0.13	0.15		0.08		
Ba	222	205	202	202	224	250	299	293	262		257		
La	17.10	8.60	8.45	8.44	16.90	11.30	23.90	23.40	20.78		19.10		
Ce	33.90	19.60	19.00	18.89	33.90	25.60	47.60	46.90	44.19		44.10		
Pr	4.30	2.70	2.63	2.56	4.31	3.58	6.02	5.94	5.70		6.05		
Nd	17.50	11.60	11.20	11.05	17.60	15.70	24.50	24.30	22.75		25.70		
Sm	3.39	2.23	2.23	2.13	3.41	3.02	4.84	4.69	4.50		4.52		
Eu	0.99	0.71	0.70	0.70	1.01	0.94	1.37	1.35	1.26		1.30		
Gd	2.62	1.72	1.67	1.61	2.73	2.13	3.52	3.45	3.52		2.92		
Tb	0.38	0.23	0.23	0.22	0.39	0.28	0.47	0.46	0.45		0.37		
Dy	2.05	1.16	1.18	1.17	2.09	1.48	2.34	2.31	2.25		1.86		
Ho	0.40	0.23	0.22	0.22	0.41	0.28	0.43	0.41	0.43		0.34		
Er	1.11	0.61	0.61	0.62	1.11	0.75	1.11	1.09	1.16		0.91		
Tm	0.16	0.09	0.09	0.08	0.16	0.11	0.15	0.15	0.16		0.12		
Yb	1.00	0.56	0.55	0.55	1.02	0.65	0.96	0.93	1.02		0.79		
Lu	0.15	0.08	0.08	0.08	0.15	0.09	0.14	0.14	0.15		0.12		
Hf	1.61	2.12	2.08	2.06	1.62	2.22	1.78	1.71	1.78		2.22		
Ta	0.09	0.05	0.05	0.06	0.09	0.06	0.09	0.09	0.08		0.06		
W	0.27	0.17	0.16	0.71	0.23	0.16	0.20	0.23	0.20		0.14		
Pb	2.77	2.46	2.39	2.42	3.03	2.81	3.42	3.38	3.06		2.61		
Th	2.33	1.16	1.13	1.14	2.39	1.32	3.25	3.14	3.05		2.20		
U	0.87	0.43	0.42	0.41	0.88	0.47	1.12	1.12	1.02		0.67		

DR7 Table 3: continued

Sample	D30-3d	D30-3d	D33-9	D33-8	D19-7	D19-6	D19-3	D19-8	D19-1	D27A-1	D27A-3a	D27A-6a	D71-3
XRF													
Y	7.6	7.6	10.6	10.2							12.4	12.5	9.5
Rb	7.4	7.4	2.9	2.8							10.7	8.2	12.8
Zn	55	55	62	61							66	65	67.3425
Cu	54	54	57	58							69	61	84
Ni	431	431	504	499							385	352	329
Sr	952	952	477	499							1360	1352	737
Zr	60	60	41	42							68	68	56.9
Cr	933	933	1665	1600							1140	1060	1228
Ba	157	157	62	62							84	90	204
V	158	158	204	194							216	221	221
La	8	8	6	7							25	23	17.5
Ce	23	23	18	18							65		31.1
Nd	13	13	13	10							44		13.9
Sc	24	24	31	28							28		33.2
ICPMS													
Li			3.06	3.54	5.96	6.07	5.23	5.68	5.62	6.31		2.98	5.10
Be			0.25	0.26	0.49	0.59	0.46	0.49	0.53	0.90		0.81	0.92
B					15.18	18.71	14.89	20.10	15.22				
Sc			20.51	15.95	37.10	36.36	38.17	36.82	36.62	21.32		29.01	31.78
V			193	191	294	292	292	288	296	292		184	200
Cr			1312.2	1334.2	105.4	97.1	121.5	102.4	120.6	3.7		656.0	1182.6
Co			67.21	67.42	37.15	37.53	38.29	37.70	39.01	27.92		46.54	60.87
Ni			541.31	538.34	52.68	52.68	54.76	52.90	57.92	32.09		337.00	304.79
Cu			58.45	60.50	117.19	118.48	121.19	119.28	124.44	137.50		54.34	87.18
Zn			60.96	61.38	77.54	77.24	79.10	76.37	80.86	74.93		63.47	60.32
Rb			2.86	2.75	11.25	11.33	12.13	11.27	12.50	9.64		7.73	13.35
Sr			492	512	1285	1296	1439	1303	1445	1898		1278	756
Y			10.95	10.53	18.91	18.93	21.96	19.38	21.04	16.35		11.95	9.61
Zr			40.75	40.51	79.57	79.73	91.13	81.20	87.97	102.57		67.58	57.51
Nb			0.56	0.58	1.14	1.13	1.30	1.16	1.28	0.80		0.51	1.87
Mo			0.32	0.32								0.31	0.66
Cs			0.03	0.04	0.05	0.05	0.06	0.05	0.06	0.10		0.05	0.17
Ba			59	62	52	53	61	52	62	124		83	203
La			6.72	6.93	25.87	25.67	30.36	25.94	30.03	33.95		22.41	15.79
Ce			14.75	15.70	73.95	73.98	84.99	73.44	86.37	95.22		61.52	32.01
Pr			2.11	2.27								9.24	4.07
Nd			9.87	10.11	47.15	46.86	55.78	47.07	55.36	53.88		38.70	16.82
Sm			2.19	2.15	7.92	7.83	9.47	7.91	9.23	8.88		6.59	3.33
Eu			0.69	0.71	2.19	2.23	2.66	2.22	2.66	2.43		1.76	0.93
Gd			1.99	2.04	5.50	5.48	6.83	5.49	6.33	5.17		4.37	2.46
Tb			0.33	0.33								0.54	0.35
Dy			2.04	1.96	4.03	4.00	5.03	4.13	4.74	3.15		2.63	1.84
Ho			0.41	0.41								0.49	0.36
Er			1.18	1.16	1.99	1.92	2.46	2.01	2.35	1.69		1.37	1.05
Tm			0.17	0.17								0.19	0.15
Yb			1.10	1.07	1.97	1.95	2.53	2.02	2.38	1.72		1.22	0.97
Lu			0.16	0.16	0.28	0.28	0.36	0.29	0.33	0.20		0.18	0.15
Hf			1.10	1.10	2.20	2.22	2.77	2.32	2.66	2.79		1.96	1.51
Ta			0.03	0.03	0.06	0.06	0.08	0.06	0.08	0.06		0.03	0.09
W			0.11	0.14								0.52	0.45
Pb			1.11	0.98	2.61	2.60	3.12	2.58	3.16	4.22		2.69	3.09
Th			0.56	0.59	1.52	1.52	1.95	1.56	1.90	2.78		1.84	2.48
U			0.22	0.22	0.54	0.56	0.66	0.55	0.70	0.85		0.56	0.94

DR7 Table 3: continued

Sample	D71-1	D71-9	D64-3	D55-4a	D17-9	D24-2	D74-4	D74-6	D17-7	D24-3	D10-4	D10-2	D2-2a
XRF													
Y	8.9	9.5	13	10.5	11.4	6.9	9.6	9.9	11.6	5.7	17.4	17.5	19.1
Rb	13.5	13.6	25.3	35.1	17.2	7.2	11.8	11.4	18.2	4.1	6.4	4.9	15.7
Zn	66.83	64.78	61.8	54.4	48	45	50.8	50.1	47	40	66	69	67
Cu	88	88	105	80	34	47	71	71	54	31	38	45	65
Ni	313	266	78	88	31	119	30	28	27	143	261	207	250
Sr	751	775	653	936	659	620	563	565	671	540	999	1284	1276
Zr	57.6	58.4	144.8	157.4	112	68	78.2	79.1	115	65	120	125	179
Cr	1133	1042	225	254	94	160	139	135	72	202	410	325	402
Ba	200	213	244	415	188	66	126	133	191	48	224	310	284
V	218	229	285	218	171	140	171	166	162	106	188	224	217
La	17.5	15.4	28.5	35.4	12	2	6.1	6.9	13	3	24	29	30
Ce	31.5	31.1	68.1	82.3	25	13	18.4	15.1	27		57	60	70
Nd	14.7	16.6	41.0	45.4	15	8	11.0	8.5	14		31	32	37
Sc	33.4	33.3	32.2	22.7	20	15	22.4	22	19		28	25	24
ICPMS													
Li	4.78	4.48	5.58	6.20	7.45	3.77	7.13	6.92	9.00	4.59	11.73	11.44	6.37
Be	0.86	0.99	0.95	1.28	0.72	0.61	1.01	1.09	0.74	0.78	0.83	0.77	1.26
B													
Sc	31.45	33.73	29.86	22.89	22.87	14.70	21.72	22.19	25.23	14.27	29.42	27.82	29.57
V	199	211	256	197	181	133	162	165	179	117	171	203	210
Cr	1072.1	1064.8	225.2	245.3	100.4	147.0	131.8	137.3	129.9	184.8	396.4	353.7	380.1
Co	57.43	54.72	28.71	25.63	20.99	22.83	20.29	20.40	19.11	23.63	43.05	40.11	42.57
Ni	285.54	253.78	77.59	84.55	35.78	131.00	30.10	30.25	38.69	167.39	300.84	253.65	275.91
Cu	90.89	92.74	106.21	81.04	31.81	46.00	67.96	67.34	52.53	35.32	36.43	41.01	63.61
Zn	59.79	60.59	54.06	50.18	52.87	45.00	48.28	49.44	50.84	38.81	65.13	71.91	68.91
Rb	13.54	14.11	26.90	37.22	18.01	7.39	11.92	11.39	19.59	4.31	5.99	4.30	16.90
Sr	757	799	658	941	668	578	538	563	684	538	1486	1928	1335
Y	9.63	10.25	14.20	10.67	11.93	7.17	10.03	10.12	11.28	6.10	18.00	18.71	18.63
Zr	57.25	60.20	141.48	153.08	104.18	62.90	73.84	74.80	113.69	63.56	118.85	127.01	174.01
Nb	1.87	1.96	2.84	3.02	2.96	1.02	0.93	0.95	2.85	0.86	10.49	11.48	12.73
Mo	0.68	0.71	0.68	0.90	0.66	0.34	0.84	0.87	0.73		0.31	0.39	0.93
Cs	0.18	0.18	0.30	0.58	0.28	0.09	0.15	0.14	0.32	0.08	0.01	0.01	0.22
Ba	204	209	239	420	194	65	130	139	193	57	218	288	267
La	15.87	17.23	29.07	34.95	12.03	5.12	6.65	6.51	12.07	4.49	25.27	27.10	31.68
Ce	32.23	34.16	65.03	76.41	26.67	12.00	15.60	15.14	29.03	10.55	56.13	60.00	72.67
Pr	4.08	4.30	8.99	10.07	3.57	1.77	2.12	2.06	3.83	1.59	7.27	7.68	9.49
Nd	16.93	17.82	38.64	41.65	14.96	8.10	9.28	9.08	16.56	6.85	29.70	31.35	38.28
Sm	3.34	3.56	7.68	7.86	3.16	1.93	2.25	2.17	3.20	1.67	5.60	5.82	6.65
Eu	0.93	0.98	2.05	2.01	0.94	0.68	0.69	0.67	0.95	0.58	1.63	1.71	2.03
Gd	2.49	2.65	5.27	4.98	2.63	1.82	2.03	1.95	2.82	1.58	4.52	4.73	5.30
Tb	0.36	0.36	0.63	0.57	0.40	0.26	0.34	0.31	0.40	0.23	0.66	0.68	0.71
Dy	1.88	1.96	2.99	2.48	2.20	1.44	1.86	1.81	2.26	1.22	3.67	3.80	3.77
Ho	0.37	0.38	0.50	0.41	0.44	0.27	0.39	0.37	0.43	0.23	0.67	0.70	0.69
Er	1.07	1.12	1.31	1.04	1.27	0.76	1.16	1.15	1.24	0.63	1.91	1.96	1.87
Tm	0.16	0.16	0.18	0.14	0.19	0.10	0.18	0.17	0.18	0.08	0.26	0.28	0.26
Yb	0.98	1.04	1.14	0.87	1.27	0.66	1.11	1.09	1.24	0.56	1.65	1.70	1.65
Lu	0.16	0.16	0.17	0.13	0.20	0.10	0.18	0.18	0.20	0.08	0.25	0.26	0.25
Hf	1.54	1.59	3.35	3.74	2.82	1.66	2.06	2.02	2.90	1.68	2.94	3.10	3.98
Ta	0.09	0.09	0.16	0.13	0.11	0.07	0.05	0.04	0.65	0.07	0.51	0.68	0.91
W	0.49	0.37	0.51	0.42	0.11	0.17	0.17	0.25	0.30		0.11	0.20	0.19
Pb	3.18	3.28	3.72	9.14	3.60	1.61	3.32	3.24	3.71	1.58	2.51	2.70	3.30
Th	2.56	2.63	3.23	5.94	1.52	0.46	0.93	0.95	1.65	0.44	2.70	2.90	2.62
U	0.95	0.97	1.20	2.26	0.67	0.22	0.54	0.53	0.69	0.20	1.16	0.76	0.91

DR7 Table 3: continued

Sample	D2-3a	D2-4	D2-3	D10-1	D4-2	D4-5	D4-7	D4-3a	D4-3	D4-6	D4-4	D12-8	D12-5
XRF													
Y	19.1			16.6	15.6	15.3	15.6	15.3	15.5	14.9	13.5	10.7	11.1
Rb	13.7			19.5	19.9	20.3	21.0	20.6	20.7	19.8	22.2	17.1	20.2
Zn	67			64	75	71	72	73	72	63	64	64	66
Cu	84			68	75	71	73	74	72	57	66	86	98
Ni	273			188	126	122	115	123	116	101	89	95	111
Sr	1269			966	1281	1272	1307	1277	1286	1314	1283	2364	2340
Zr	185			133	178	178	177	179	178	175	178	202	190
Cr	408			298	188	223	167	184	175	164	164	144	149
Ba	285			264	320	308	319	310	312	322	337	391	401
V	219			195	200	196	196	196	195	178	175	177	177
La	32			26	30	30	32	31	31	31	31	32	33
Ce	74			57	69	66	71	65	75	67	70	79	82
Nd	38			29	36	34	36	36	36	34	35	43	43
Sc	24			23	18	19	18	19	19	15	16	16	13
ICPMS													
Li	5.57	7.63	7.43	11.14				8.48		9.63			6.00
Be	1.31	1.42	1.26	1.01				1.37		1.33			1.18
B		14.41	16.52										
Sc	28.65	20.41	19.64	25.76				22.56		21.19			14.80
V	217	242	219	185				196		177			164
Cr	482.6	47.5	67.9	294.2				170.9		167.7			154.9
Co	43.58	26.89	23.99	36.44				32.19		28.50			26.61
Ni	302.04	43.13	39.06	216.20				140.17		117.93			124.49
Cu	81.08	130.97	113.66	64.61				72.45		54.98			89.60
Zn	69.93	68.92	61.49	62.22				73.74		68.17			65.28
Rb	14.69	17.99	17.29	17.01				22.41		20.92			17.86
Sr	1325	1654	1542	1437				1339		1345			3406
Y	18.48	19.34	17.43	17.32				15.41		15.19			11.65
Zr	179.56	197.09	175.41	132.40				174.53		171.03			193.98
Nb	12.91	13.74	12.85	10.86				14.91		14.31			10.93
Mo	0.87			0.72				1.07		0.96			0.77
Cs	0.21	0.22	0.22	0.21				0.23		0.26			0.22
Ba	272	320	299	265				291		324			385
La	32.55	34.51	31.82	25.15				32.10		32.41			37.03
Ce	75.45	82.49	76.41	55.70				71.44		70.87			85.44
Pr	9.86			7.15				9.26		9.13			11.07
Nd	39.53	42.21	37.76	29.00				37.04		36.15			43.56
Sm	6.82	7.38	6.66	5.43				6.50		6.24			7.16
Eu	2.05	2.22	2.03	1.56				1.95		1.84			1.92
Gd	5.39	5.57	4.96	4.35				5.10		4.82			4.59
Tb	0.72			0.63				0.65		0.63			0.56
Dy	3.74	3.97	3.55	3.54				3.29		3.16			2.68
Ho	0.69			0.65				0.58		0.56			0.45
Er	1.89	2.01	1.82	1.82				1.52		1.49			1.12
Tm	0.26			0.25				0.21		0.20			0.15
Yb	1.65	1.82	1.69	1.59				1.24		1.24			0.90
Lu	0.25	0.27	0.25	0.24				0.19		0.19			0.14
Hf	4.14	4.45	3.97	3.10				4.19		4.14			4.66
Ta	0.93	0.83	0.76	0.64				1.10		1.07			0.51
W	0.23			0.25				0.25		<0.07			0.16
Pb	3.39	4.26	3.92	2.52				3.51		3.84			5.00
Th	2.71	3.04	2.83	2.68				3.03		3.31			4.49
U	0.94	1.17	1.11	0.74				0.92		1.16			1.31

DR7 Table 3: continued

Sample	D5-7	D4-3a	D4-3b	D8-3	D9-2
XRF					
Y	18.6			15.2	14.6
Rb	131.1			33.8	35.2
Zn	87			54	54
Cu	119			92	92
Ni	4			76	72
Sr	1356			791	783
Zr	136			151	154
Cr	2			214	219
Ba	577			448	448
V	157			200	200
La	13			21	20
Ce	38			51	50
Nd	23			27	29
Sc	10			23	22
ICPMS					
Li	23.65	11.92	8.41	7.26	5.92
Be	2.12	1.77	1.18	1.13	1.08
B		14.96	11.71		
Sc	12.80	13.02	9.82	28.27	27.24
V	174	243	169	201	196
Cr	26.1	3.4	8.4	237.1	220.1
Co	13.66	18.99	13.23	30.33	29.01
Ni	4.26	10.37	8.10	94.11	85.90
Cu	113.03	125.68	90.54	90.48	90.10
Zn	94.09	81.16	54.65	68.05	61.03
Rb	137.47	30.37	22.07	29.65	31.42
Sr	1352	1081	1323	1149	1147
Y	18.81	19.56	14.09	15.80	15.50
Zr	127.77	247.41	176.12	151.95	151.70
Nb	4.57	21.21	15.36	4.22	4.21
Mo	0.76			0.91	0.92
Cs	1.05	0.38	0.27	0.42	0.45
Ba	381	410	327	407	445
La	16.06	42.62	31.66	22.49	22.49
Ce	38.10	94.22	70.56	51.56	51.15
Pr	5.43			6.92	6.82
Nd	24.02	45.76	33.87	28.82	28.60
Sm	5.33	8.02	5.87	5.77	5.75
Eu	1.72	2.28	1.73	1.47	1.45
Gd	5.01	6.03	4.30	4.56	4.43
Tb	0.70			0.62	0.61
Dy	3.79	4.07	2.89	3.23	3.21
Ho	0.71			0.58	0.57
Er	1.94	1.91	1.42	1.64	1.59
Tm	0.27			0.23	0.22
Yb	1.68	1.74	1.24	1.43	1.43
Lu	0.25	0.24	0.18	0.22	0.22
Hf	3.40	5.63	4.03	3.84	3.78
Ta	0.34	1.30	0.94	0.27	0.27
W	<0.07			0.13	0.23
Pb	8.82	5.51	3.98	4.76	4.79
Th	1.43	4.59	3.32	3.35	3.31
U	0.59	1.47	1.09	1.18	1.22

DR7 Table 3: continued

Sample	$^{87}Sr/^{86}Sr$	$^{143}Nd/^{144}Nd$	εNdm	$^{147}Sm/^{144}Nd$	$^{206}Pb/^{204}Pb$	$^{207}Pb/^{204}Pb$	$^{208}Pb/^{204}Pb$	$^{176}Hf/^{177}Hf$	εHfm
D36-3	0.702767	0.513085	8.72	0.110	18.838	15.521	38.325		
D33-8	0.702728	0.513093	8.88	0.123	18.814	15.517	38.304		
D22-2	0.702714	0.513079	8.60	0.117	18.840	15.527	38.362	0.283139	12.98
D30-10	0.702664	0.513086	8.74	0.116	18.842	15.531	38.374		
D15-4	0.702885	0.513045	7.94	0.120	18.950	15.535	38.435	0.283134	12.80
D30-3a	0.702672	0.513094	8.90	0.106	18.867	15.531	38.381		
D33-8	0.702728	0.513093	8.88	0.129	18.814	15.517	38.304		
D19-3	0.702619	0.513085	8.72	0.103	18.673	15.513	38.194		
D27A-6a	0.702737	0.513067	8.37	0.103	18.711	15.513	38.221	0.283144	13.16
D71-9	0.702632	0.513017	7.39	0.121	18.985	15.537	38.444	0.283123	12.41
D55-4a					18.906	15.552	38.434		
D24-3	0.702930	0.513053	8.10	0.148	18.727	15.525	38.287		
D10-2	0.703127	0.513029	7.63	0.112	18.843	15.552	38.467		
D2-3a	0.703132	0.513021	7.47	0.104	18.822	15.551	38.432		
D4-6	0.702986	0.513018	7.41	0.104	18.869	15.551	38.457		
D12-8	0.702963	0.513034	7.72	0.099	18.855	15.555	38.447		
D8-3	0.703208	0.513045	7.94	0.121	18.890	15.552	38.461		
D9-2	0.703193	0.513027	7.59	0.121	18.895	15.552	38.465		

DR8 Table 4: Sr-Nd-Hf-Pb isotopic dataset of dredged volcanic rocks. Typical in-run precision (2se) are ±0.000010 ($^{143}Nd/^{144}Nd$), ±0.000016 ($^{87}Sr/^{86}Sr$) and ±0.000008 ($^{176}Hf/^{177}Hf$). External (2sd) precision is ±0.000028, ±0.000012 and ±0.000015, respectively. Pb-isotopes have an external precision (2sd) of ±0.04-0.06% for $^{206}Pb/^{204}Pb$ and $^{207}Pb/^{204}Pb$, and 0.07-0.09% for $^{208}Pb/^{204}Pb$.

Sample	Voyage	Dredge N°	Rock type	Location	Magmatic Suite	$^{87}Sr/^{86}Sr$	$^{143}Nd/^{144}Nd$	εNd_m
D18-4	SS10/04	D18	wholerock	Monzier Rift	BABB	0.703642	0.512876	4.64
D20-6	SS10/04	D20	wholerock	Monzier Rift	BABB	0.702881	0.513088	8.78
D21-1a	SS10/04	D21	glass	Monzier Rift	BABB	0.702951	0.513050	8.04
D25-2	SS08/06	D25	glass	Monzier Rift	BABB	0.703075	0.513027	7.59
D28-7	SS08/06	D28	glass	Monzier Rift	BABB	0.703428	0.512988	6.83
D74A-3	SS03/09	D74A	wholerock	Monzier Rift	BABB	0.702959	0.513019	7.43
D29-1	SS10/04	D29	wholerock	Monzier Rift	Low K arc lava	0.703038	0.513036	7.76
D24-2	SS08/06	D24	wholerock	Monzier Rift	Low K arc lava	0.702857	0.513066	8.35
D27-5	SS08/06	D27	glass	Monzier Rift	Low K arc lava	0.702983	0.513117	9.34
D29-1	SS08/06	D29	wholerock	Monzier Rift	Low K arc lava	0.703101	0.513058	8.19
D29-2	SS08/06	D29	wholerock	Monzier Rift	Low K arc lava	0.702826	0.513086	8.74
D31-7	SS08/06	D31	wholerock	Monzier Rift	Low K arc lava	0.702791	0.513109	9.19
D32-7	SS08/06	D32	wholerock	Monzier Rift	Low K arc lava	0.702848	0.513093	8.88
D33-5	SS08/06	D33	wholerock	Monzier Rift	Low K arc lava	0.702779	0.513131	9.62
D8-2	SS10/04	D8	wholerock	Monzier Rift	Med K arc lava	0.702819	0.513066	8.35
D11-2	SS10/04	D11	wholerock	Monzier Rift	Med K arc lava	0.702832	0.513062	8.27
D14-3	SS10/04	D14	wholerock	Monzier Rift	Med K arc lava	0.702935	0.513089	8.80
D15-7a	SS10/04	D15	wholerock	Monzier Rift	Med K arc lava	0.702753	0.513088	8.78
D24-1	SS10/04	D24	wholerock	Monzier Rift	Med K arc lava	0.702874	0.513009	7.24
D27-3	SS10/04	D27	wholerock	Monzier Rift	Med K arc lava	0.702906	0.513059	8.21
D26-4	SS08/06	D26	wholerock	Monzier Rift	Med K arc lava	0.702874	0.513070	8.43
D30-8	SS08/06	D30	wholerock	Monzier Rift	Med K arc lava	0.702673	0.513092	8.86
D31-1a	SS08/06	D31	wholerock	Monzier Rift	Med K arc lava	0.702723	0.513093	8.88

DR9 Table 5: Sr-Nd of Monzier Rift back-arc basalts and low- to medium K_2O lavas. Major and trace elements and Pb-isotopes can be found in Patriat et al., (2019). BABB= back-arc basalt. (see caption Table 5 for further details)